Cyclin A2 localises in the cytoplasm at the S/G2 transition to activate PLK1

Helena Silva Cascales[1], Kamila Burdova[2], Anna Middleton[1], Vladislav Kuzin[1], Erik Müllers[1], Henriette Stoy[1], Laura Baranello[1], Libor Macurek[2], Arne Lindqvist[1*]

*Corresponding author:
Arne Lindqvist
Department of Cell and Molecular Biology
Karolinska Institutet
Stockholm, Sweden
Phone: +46-8-52487309
E-mail: arne.lindqvist@ki.se

Affiliations
1. Department of Cell and Molecular Biology; Karolinska Institutet; Stockholm, Sweden.
2. Laboratory of Cancer Cell Biology; Institute of Molecular Genetics; Academy of Sciences of the Czech Republic; Prague, Czech Republic.

Keywords: Cyclin A2, PLK1, Bora, Cell cycle, DNA damage, CDK1, CDK2, p21,

Abstract

Cyclin A2 is a key regulator of the cell cycle, implicated both in DNA replication and mitotic entry. Cyclin A2 participates in feedback loops that activate mitotic kinases in G2-phase, but why active Cyclin A2-CDK2 during S phase does not trigger mitotic kinase activation remains unclear. Here we describe a change in localisation of Cyclin A2 from being only nuclear to both nuclear and cytoplasmic at the S/G2 border. We find that Cyclin A2-CDK2 can activate the mitotic kinase PLK1 through phosphorylation of Bora, and that only cytoplasmic Cyclin A2 interacts with Bora and PLK1. Expression of predominately cytoplasmic Cyclin A2 or phospho-mimicking PLK1 T210D can partially rescue a G2 arrest caused by Cyclin A2 depletion. Cytoplasmic presence of Cyclin A2 is restricted by p21, in particular after DNA damage. Cyclin A2 chromatin association during DNA replication and additional mechanisms contribute to Cyclin A2 localisation change in G2 phase. We find no evidence that such mechanisms involve G2 feedback loops and suggest that cytoplasmic appearance of Cyclin A2 at the S/G2 transition functions as a trigger for mitotic kinase activation.

Synopsis

Main mitotic kinases as PLK1 are activated at the S/G2 transition. A change in Cyclin A2 localisation at the S/G2 transition enables activation of PLK1.

Main points

-Cyclin A2 appears in the cytoplasm at the S/G2 transition

-Association with replicating chromatin and p21 restricts Cyclin A2 to the nucleus

-DNA damage ensures nuclear Cyclin A2 through p21

-Cytoplasmic Cyclin A2 initiates PLK1 activation

Introduction

Correct progression through the cell cycle depends on the tight regulation of Cyclin-CDK complexes over time. Sequential waves of Cyclin dependent kinase (CDK) activity ensure timely phosphorylation of a large number of substrates. CDK activity increases through the cell cycle, allowing separation of high-affinity sites that initiate early events as onset of DNA replication, and low-affinity sites that enable late events as mitosis (Swaffer et al., 2016). On top of this general trend, different Cyclin-CDK complexes can selectively phosphorylate target proteins, both by different affinity to a target and by being present at different cellular locations (Örd and Loog, 2019). For example, although both Cyclin A2 (CycA2) and Cyclin B1 (CycB1) have been implicated in mitotic entry, CycA2 appears mostly nuclear, whereas CycB1 appears mainly in the cytoplasm (Pines and Hunter, 1991).

Due to its presence during S, G2, and early mitosis, CycA2 is at a strategic position to control a large part of the cell cycle (Pagano et al., 1992; Fung et al., 2007). Indeed, CycA2 regulates multiple aspects of S-phase by steering phosphorylation of key components as CDC6 (Petersen et al., 1999), pre-replication complexes (Furuno et al., 1999; Katsuno et al., 2009), and components of the replication machinery (Cardoso et al., 1993; Frouin et al., 2005). Depletion of CycA2 leads to an arrest in G2-phase, which could be suspected due to errors in completing DNA replication (Fung et al., 2007; Gong and Ferrell, 2010; Gong et al., 2007; Oakes et al., 2014; De Boer et al., 2008). However, recent data show that depletion of CycA2 specifically in G2-phase blocks mitotic entry. Interestingly, similar depletion of CycB1 does not block mitotic entry, but rather affects later mitotic progression (Hégarat et al., 2020). This shows that apart from its functions during S-phase, CycA2 is a key player in regulating progression into mitosis.

During G2-phase, CycA2 stimulates transcription and represses degradation of multiple mitotic regulators (Oakes et al., 2014; Hein and Nilsson, 2016; Laoukili et al., 2008; Lukas et al., 1999). As the mitotic regulators accumulate, CycA2 participates in the feedback-loops that culminate in full CDK1 activation and mitotic entry (Mitra and Enders, 2004). A key player in these feedback-loops is Polo-like kinase 1 (PLK1) (Lindqvist et al., 2009). We and others previously showed that PLK1 is activated by Aurora A, in a reaction that requires the cofactor Bora (Macurek et al., 2008; Seki et al., 2008). CDK-mediated phosphorylation of Bora facilitates PLK1 activation, and both CycA2- and CycB1-containing complexes have been suggested to phosphorylate Bora (Gheghiani et al., 2017; Vigneron et al., 2018; Parrilla et al.,

2016; Thomas et al., 2016). Interestingly, Bora appears exclusively cytoplasmic, raising the possibility that a cytoplasmic Cyclin-CDK activates PLK1 (Feine et al., 2014; Bruinsma et al., 2015).

Although CycA2 targets are mostly nuclear, CycA2 has been shown to also regulate events in the cytoplasm, particularly after S-phase. This includes loading of Eg5 to centrosomes in G2-phase and inhibiting endocytic vesicle fusion to control membrane transport as cells enter into mitosis (Woodman et al., 1993; Kanakkanthara et al., 2016; Li et al., 2018). CycA2 appears predominantly nuclear but can shuttle between nucleus and cytoplasm, despite not possessing a classical NLS (Jackman et al., 2002). CycA2 association with different proteins has been described to affect localisation both to the nucleus and to the cytoplasm (Maridor et al., 1993; Tsang et al., 2007; Bendris et al., 2011). However, the exact mechanism that regulates CycA2 localisation remains elusive. In addition, whether CycA2 localisation changes through the cell cycle and impacts on cell cycle progression remains unclear.

Here we characterise CycA2 localisation through the cell cycle and describe that CycA2 appears in the cytoplasm at the S/G2 transition. We find that cytoplasmic CycA2 activates PLK1 through phosphorylation of Bora. We further describe that cytoplasmic localisation of CycA2 is abolished in response to DNA damage in a manner that depends on p21. The cytoplasmic appearance of CycA2 depends on multiple mechanisms, including CycA2 association with chromatin during DNA replication. We find no evidence that these mechanisms involve feedback-loops involved in PLK1 and CDK1 activation, raising the possibility that cytoplasmic localisation of CycA2 functions as a trigger for mitotic kinase activation.

102 ## Results

103 **Cyclin A2 accumulates in the cytoplasm at the S/G2 transition**

104 In order to study the dynamics of CycA2 in live cells we targeted *CCNA2* using rAAV-
105 mediated homologous recombination. We introduced an ORF for EYFP in the *CCNA2* locus of
106 U2OS (Akopyan et al., 2014) and RPE cell lines to create a CycA2-eYFP fusion protein (Fig 1A
107 and S1A,B). Western blot analysis confirmed the successful integration of the eYFP ORF in
108 one of the two alleles of CycA2 as we detected a band that migrated at the predicted size of
109 endogenous untagged CycA2 and a band that migrated at the predicted size of the CycA2-
110 eYFP fusion protein (Fig S1A). Importantly, siRNA to target CycA2, addition of S-trityl-L-
111 cysteine (STLC), or addition of etoposide showed a similar behaviour of both bands as to
112 CycA2 in parental RPE cells, indicating that eYFP was specifically introduced at the *CCNA2*
113 locus (Fig S1A). Similar to in U2OS cells, CycA2-eYFP in RPE cells is present in all cells from
114 early S-phase and its levels increase over time reaching a maximum at mitosis when CycA2 is
115 rapidly degraded (Fig 1A and S1B) (Akopyan et al., 2014).
116
117 To monitor CycA2-eYFP localisation, we followed RPE-CycA2-eYFP and U2OS-CycA2-eYFP
118 cells by time-lapse microscopy (Fig 1A and S1B). In all cells, CycA2-eYFP was first visible in
119 the nucleus, but also appeared in the cytoplasm approximately 4h before mitosis (Fig 1B).
120 We next treated RPE CycA2-eYFP cells with a short pulse of EdU to mark cells in S-phase, and
121 quantified immunofluorescence stainings. Whereas CycA2-eYFP was present in the nucleus
122 in all cells once expressed, cells positive for cytoplasmic CycA2-eYFP contained 4n DNA
123 content and low EdU staining (Fig S1C). A similar pattern was found when labelling the
124 parental RPE cells, using an antibody to detect endogenous CycA2 (Fig S1D). We note that
125 CycA2-eYFP showed a slightly higher expression in the cytoplasmic fraction compared to
126 CycA2. However, although the magnitude of cytoplasmic accumulation may differ, the
127 pattern and timing of cytoplasmic appearance is similar for CycA2 and CycA2-eYFP, showing
128 that CycA2-eYFP can be used to study CycA2 localisation (Fig 1C, D, and S1C, D).
129
130 In order to pinpoint the position in the cell cycle when cells start to accumulate cytoplasmic
131 CycA2, we estimated a time-course by sorting cells for increasing CycA2 or CycA2-eYFP levels
132 and DAPI content (Akopyan et al., 2014, 2016). Interestingly, we found that CycA2-eYFP
133 appeared in the cytoplasm at the time when a decrease in EdU incorporation was apparent
134 (Fig 1C). A similar pattern was found when assessing CycA2 levels in parental RPE cells (Fig
135 1C). If CycA2 appears in the cytoplasm after completion of S-phase, we reasoned that

136 blocking progression through S-phase would inhibit cytoplasmic appearance of CycA2. We
137 therefore treated RPE-CycA2-eYFP cells with thymidine or hydroxyurea and quantified the
138 proportion of cells that accumulate CycA2-eYFP in the cytoplasm (Fig 1E). The treatment
139 with either drug resulted in a decreased number of cells accumulating CycA2-eYFP in the
140 cytoplasm, suggesting that cells blocked in S-phase do not gain cytoplasmic CycA2-eYFP.
141 Thus, CycA2 appears in the cytoplasm at the S/G2 transition and gradually increases in the
142 cytoplasm through G2-phase.
143
144 **CycA2 regulates the S/G2 transition**
145 We next sought to test whether cytoplasmic appearance of CycA2 impacts on cell cycle
146 progression. CycA2 has functions through both S and G2-phases and in accordance with
147 previous reports, we find that knockdown of CycA2 leads to accumulation of 4N cells.
148 To separate events in S-phase and G2, we depleted CycA2 by siRNA and monitored S-phase
149 progression by a PCNA chromobody and PLK1 activation by a FRET-based biosensor
150 (Akopyan et al., 2014). Whereas control cells showed PLK1 activation as PCNA foci sharply
151 decreased at the S/G2 border, CycA2 depleted cells showed no sharp decrease in PCNA foci.
152 Rather, the amount and intensity of PCNA foci gradually decreased, and PLK1 activity
153 remained low (Fig 2A, B). This shows that PLK1 activation is impaired after CycA2 depletion,
154 but also suggests that the S/G2 transition is impaired in the absence of CycA2. To test
155 whether cytoplasmic CycA2 can rescue cell cycle progression after depletion of endogenous
156 CycA2, we constructed siRNA-resistant versions of CycA2 (CycA2-NT) tagged to mCherry,
157 including either 3 NES sequences or 6 NLS sequences (Fig 2C). We used inducible expression
158 of the CycA2 constructs in $p53^{-/-}$ RPE cells to avoid possible nuclear relocation due to p53-
159 p21 activation after CycA2 siRNA (see below). Although both CycA2-mCherry 3xNES and
160 6xNLS are not restricted from nucleo-cytoplasmic shuttling, we find that upon induction,
161 CycA2-mCherry 3xNES appears predominately in the cytoplasm and CycA2-mCherry 6xNLS
162 appears predominately in the nucleus (Fig 2D). We find that both constructs partially
163 rescued a cell cycle delay after CycA2 siRNA, suggesting that the CycA2 siRNA phenotype
164 depends on a reduction of CycA2 levels (Fig 2E). Interestingly, expression of CycA2-mCherry
165 3xNES stimulated mitotic entry earlier than CycA2-mCherry 6xNLS, which would be
166 consistent with a function for cytoplasmic CycA2 in stimulating cell cycle progression.
167
168 **Cytoplasmic CycA2 triggers PLK1 activation**

169 CycA2 is recently suggested to promote mitotic entry by activation of PLK1 (Vigneron et al.,
170 2018; Gheghiani et al., 2017). As depletion of CycA2 resulted in a loss of PLK1 activation, but
171 also suggested that S-phase completion may be impaired (Fig 2A, B), we sought to
172 investigate the contribution of Cyclin-CDK complexes after the S/G2 transition. To this end,
173 we added inhibitors to CDK1 or CDK2 to cells in G2-phase and monitored PLK1 activation.
174 We find that addition of either CDK1 or CDK2 inhibitor disturbed PLK1 activity as well as the
175 pT210 modification of PLK1, showing the most prominent effect with a combination of both
176 inhibitors (Fig 3A, B). This suggests that CDK activity is important for PLK1 activation during
177 G2-phase. Indeed, Aurora A-mediated phosphorylation of PLK1 was further stimulated by
178 CycA2-CDK2 activity in the presence of Bora (Fig 3C). Similarly, we find that CycA2-CDK2 was
179 able to phosphorylate Bora at a Thr-Pro motif and possibly other residues *in vitro* (Fig 3D).
180 To assess if and where CycA2 forms a complex with PLK1 and Bora, we immunoprecipitated
181 CycA2 from nuclear or cytoplasmic extracts of G2 cells and probed for interactors.
182 Interestingly, we found that both Bora and PLK1 co-immunoprecipitated with CycA2
183 specifically in the cytoplasmic fraction of G2 synchronised cells (Fig 3E). Similarly, an
184 interaction between Bora and PLK1 was detected exclusively in the cytoplasm (Fig 3F). Thus,
185 CycA2-CDK2 can activate PLK1 *in vitro* and the interactions required for CycA2-mediated
186 PLK1 activation are detected in the cytoplasm, but not in the nucleus.
187
188 To test the importance of CycA2-mediated PLK1 activation for cell cycle progression, we
189 monitored mitotic entry in a U2OS cell line with inducible expression of PLK1 containing the
190 phospho-mimicking substitution T210D. Induction of PLK1 T210D did not affect the rate of
191 mitotic entry, suggesting that phosphorylation of T210 is not a rate-limiting factor for mitotic
192 entry. After transfection of siRNA to CycA2, mitotic entry was impaired. Importantly, we
193 found that induced expression of PLK1 T210D partially rescued mitotic entry after CycA2
194 siRNA, suggesting that CycA2 stimulates mitotic entry in part by activating PLK1 (Fig 3G).
195 Thus, although CycA-CDK is active through S-phase, PLK1 activation is detected
196 simultaneously as CycA2 appears in the cytoplasm at the S/G2 transition. Depletion of CycA2
197 prohibits PLK1 activation, but mitotic entry can be partially rescued by expression of largely
198 cytoplasmic CycA2 or by active PLK1. Inhibition of CDK activity reduces PLK1 activation in G2-
199 phase and interactions between CycA2, Bora, and PLK1 are detected in the cytoplasm but
200 not in the nucleus. Taken together, our results indicate that cytoplasmic CycA2 plays a key
201 role in the initial activation of PLK1 during G2.
202

203 **Cytoplasmic accumulation of CycA2 is not triggered by mitotic kinases**
204 The observation that CycA2-eYFP only accumulates in the cytoplasm after S-phase
205 completion suggests that cytoplasmic localisation is suppressed during S-phase or stimulated
206 during G2-phase. We previously showed that mitotic-inducing activities of CDK1 and PLK1
207 start to accumulate at the S/G2 transition (Akopyan et al., 2014). However, we find no
208 evidence that addition of inhibitors to PLK1 or its upstream kinase Aurora A affects
209 cytoplasmic appearance of CycA2 (not shown). Addition of inhibitors to CDK1 or CDK2 led to
210 a slight decrease in cells accumulating cytoplasmic CycA2-eYFP, but interpretation of these
211 results is hampered by that CDK inhibition may affect S-phase progression (not shown). To
212 assess the contribution of CDK1/2 activity to the cytoplasmic localisation of CycA2-eYFP
213 specifically in G2-phase, we followed individual cells that had a low but clear presence of
214 CycA2-eYFP in the cytoplasm at the time of addition of inhibitors. To improve comparison,
215 we synchronised these cells *in silico* at the time point when each cell reaches a certain level
216 of cytoplasmic CycA2-eYFP (Fig S2A). We did not observe significant differences in the
217 dynamics of cytoplasmic accumulation of CycA2-eYFP in either of the treatments, showing
218 that a reduction of CDK1/2 activity does not compromise cytoplasmic accumulation of
219 CycA2-eYFP once initiated (Fig S2A).
220
221 To test if CDK1/2 activity could promote the onset of cytoplasmic accumulation of CycA2-
222 eYFP, we increased CDK activity using a Wee1 inhibitor. Wee1 inhibition increased the
223 amount of mitotic cells and decreased the duration between cytoplasmic appearance of
224 CycA2-eYFP and mitotic entry, suggesting that CDK activity is increased and that G2-phase is
225 therefore shortened. However, we did not detect an increased rate of cytoplasmic
226 appearance of CycA2-eYFP after Wee1 inhibition (Fig S2B). Thus, we find no evidence that
227 CDK1/2 activity regulates CycA2 appearance in the cytoplasm at the S/G2 transition.
228
229 **Lack of CDK1 can lead to loss of cytoplasmic CycA2**
230 Given the lack of evidence for key G2 kinase activities to modulate CycA2 localisation, we
231 reasoned that perhaps a change in binding partner could explain CycA2 cytoplasmic
232 localisation. CycA2 is described to complex predominately with CDK2 in S-phase and
233 increasingly with CDK1 as cells approach mitosis (Merrick et al., 2008). Furthermore, while
234 CDK2 is mostly nuclear, CDK1 is present both in the nucleus and in the cytoplasm (Moore et
235 al., 1999; Pines and Hunter, 1991, 1994), therefore potentially providing a mechanism to
236 regulate CycA2 localisation.

237

238 To investigate the involvement of CDK-Cyclin complex formation in the localisation of CycA2
239 we used siRNAs to target either CDK1 or CDK2 (Fig S2C). Live-cell imaging of RPE CycA2-eYFP
240 cells after CDK1 or CDK2 knockdown revealed reduced numbers of cells going through
241 mitosis. Further, CDK1 knockdown increased mitotic duration, showing that knockdown of
242 either CDK affected cell cycle progression (Fig S2D). Analysis of quantitative
243 immunofluorescence in single cells revealed that knock down of CDK1 led to an increase in
244 the number of cells in G2, presumably due to a lengthening of G2-phase, and subsequently,
245 to the amount of cells with cytoplasmic CycA2 (Fig 4A, B). Interestingly, a subset of G2 cells
246 contained high nuclear CycA2 and low cytoplasmic CycA2 levels, indicating that CDK1 may
247 facilitate the localisation of CycA2 to the cytoplasm (Fig 4A, arrows; Fig 4B, grey triangle). On
248 the other hand, CDK2 knockdown led to a marked decrease in number of cells in G2-phase,
249 explaining the reduced level of CycA2 and CDK1 at a population level (Fig 4A, B and S2C).
250 However, contrary to the observation after CDK1 depletion, the relation between nuclear
251 and cytoplasmic CycA2 was similar after CDK2 and control knockdown (Fig 4B). Given that
252 knockdown of CDK1 decreased cytoplasmic Cyclin A2 levels, we sought to test if Cdk1 binds
253 to cytoplasmic CycA2 and CDK2 binds to nuclear CycA2. However, we find that both CDK1
254 and CDK2 are present in both nuclear and cytoplasmic CycA2 and CycA2-eYFP
255 immunoprecipitates (Fig 4C). Thus, although we cannot exclude the possibility that CycA2
256 localisation is affected by a stress response associated with depletion of a key cell cycle
257 regulator (see below), our data shows that depletion of CDK1 can impair the cytoplasmic
258 localisation of CycA2 in G2-phase. However, as cytoplasmic CycA2 exists in complex with
259 both CDK1 and CDK2, we conclude that the cytoplasmic appearance of CycA2 cannot be
260 explained solely by association with CDK1.

261

262 **CycA2 associates with chromatin during S-phase**

263 We next sought to test if CycA2 is restricted to the nucleus during S-phase. The defining
264 process of S-phase is replication of DNA, and Cyclin A2 has been reported to associate
265 directly with the replication protein PCNA (Koundrioukoff et al., 2000; Cardoso et al., 1993;
266 Frouin et al., 2005). We therefore synchronised RPE-CycA2-eYFP cells by addition of
267 Hydroxyurea (HU) and assessed the chromatin association of CycA2-eYFP using Chromatin
268 immunoprecipitation (ChIP) followed by qPCR at 5 chromosomal locations: 2 expressed
269 promoter regions (A, MYC and B, IRF1), one origin of replication (C, LAMB2 (Abdurashidova
270 et al., 2000)), the alpha-satellite region (D) and an intragenic region on Chromosome 1 (E).

271 We compared the chromatin binding pattern of CycA2-eYFP at early replicated regions (i.e.
272 expressed genes) and regions undergoing late replication (gene desert areas). When cells
273 approached mid S-phase 4h after HU washout we detected an increase in CycA2-eYFP
274 chromatin binding at the expressed genomic locations (A, B and C in Fig 5A), while we did
275 not find a significant increase at the α-satellite and intragenic regions. Interestingly, the
276 chromatin association of CycA2-eYFP decreased 8h after release from HU, at a time when
277 many of the cells had completed DNA replication (Fig 5A). This suggests that CycA2-eYFP
278 association with chromatin is increased during ongoing DNA replication. We therefore
279 sought to test whether CycA2-eYFP chromatin association restricted CycA2-eYFP mobility in
280 the nucleus. To this end, we used fluorescence recovery after photobleaching (FRAP), and
281 compared the nuclear recovery of RPE-CycA2-eYFP cells expressing CycA2-eYFP only in the
282 nucleus (S-phase) or in both nucleus and cytoplasm (G2-phase). To avoid overstating the
283 immobile fraction due to bleaching and focus changes, we normalised the bleached region
284 to an unbleached area in the same nucleus. Although the recovery of fluorescence was
285 somewhat slower in S-phase versus in G2-phase, we found no major difference between the
286 recovery curves, suggesting that the mobility of CycA2-eYFP is not dramatically altered
287 between S and G2-phases. Moreover, in contrast to PCNA that shows a large immobile
288 fraction in replication foci (Trembecka-Lucas et al., 2013), the immobile component of
289 CycA2-eYFP is limited during both S- and G2-phases (Fig 5B). This suggests that a majority of
290 CycA2 is not stably bound to chromatin. Indeed, using protein fractionation instead of ChIP,
291 we do not detect a marked decrease of CycA2 in the insoluble – chromatin bound – fraction
292 at late times after release from HU. Rather, whereas both CycA2 and CycA2-eYFP increase in
293 the cytoplasmic fraction, their component in the insoluble fractions remains unaltered (Fig
294 5C). Taken together, this indicates that CycA2-eYFP associates more with replicating
295 chromatin, but also that CycA2 cytoplasmic appearance at the S/G2 transition cannot be
296 explained by a decrease in chromatin association. Rather, CycA2 chromatin association
297 remains similar as total and cytoplasmic CycA2 levels increase through G2-phase.
298
299 **The DNA damage response modulates cytoplasmic accumulation of CycA2 through p21**
300 DNA replication functions as a brake on cell cycle progression by limiting activities that
301 promote mitosis (Lemmens et al., 2018; Saldivar et al., 2018). A similar limitation of activities
302 that promote mitosis is achieved by DNA damage. At least for certain signalling components,
303 S-phase resembles a low-level DNA damage response (Lemmens and Lindqvist, 2019;
304 Sørensen and Syljuåsen, 2012). We therefore sought to test whether the occurrence of

305 cytoplasmic CycA2 is affected by DNA damage. After addition of the radiomimetic drug
306 Neocarzinostatin (NCS) or of the Topoisomerase II inhibitor Etoposide, cytoplasmic CycA2-
307 eYFP signal disappeared (Fig 6A-C, and S3A). The reduction in cytoplasmic CycA2-eYFP
308 occurred between 2 and 5h after NCS or Etoposide addition and was mirrored by a rapid
309 increase in nuclear fluorescence. Such an increase in nuclear fluorescence was only detected
310 in cells containing cytoplasmic CycA2-eYFP (Fig 6B). Further, the loss of cytoplasmic
311 fluorescence and the increase in nuclear fluorescence was not affected by addition of a
312 proteasome inhibitor (Fig 6C), indicating that upon DNA damage, cytoplasmic Cyclin A2
313 translocates to the nucleus. As a consequence, the nuclear fluorescence in G2 cells exposed
314 to NCS or Etoposide exceeded the nuclear fluorescence observed during an unperturbed G2-
315 phase (Fig 6C).
316
317 A few hours after loss of CycA2-eYFP in the cytoplasm, CycA2-eYFP signal disappeared also
318 from the nucleus (Fig 6A-C). In contrast to cytoplasmic CycA2-eYFP signal, nuclear CycA2-
319 eYFP signal remained after addition of a proteasome inhibitor, suggesting that nuclear
320 CycA2-eYFP loss involves protein degradation (Fig 6C). The loss of cytoplasmic CycA2-eYFP
321 occurred at similar time-scales after DNA damage as what we and others previously
322 described for p53- and p21-dependent nuclear translocation of CycB1-eYFP (Mullers et al.,
323 2014; Krenning et al., 2014; Johmura et al., 2014). Moreover, loss of nuclear CycA2-eYFP was
324 apparent in cells receiving DNA damage in G2-phase, but was rarely visible in cells targeted
325 in S-phase, which would be consistent with a role for p21, whose expression is suppressed
326 during S-phase despite the presence of damaged DNA (Fig 6A, B) (Müllers et al., 2017; Sheng
327 et al., 2019). To test whether p53-p21 affects CycA2 localisation, we transfected cells with
328 either p21 or p53 siRNAs for 48 h and assessed the dynamics of CycA2-eYFP upon DNA
329 damage. Interestingly, p21 and p53 knockdown impaired both the cytoplasmic and
330 subsequent nuclear loss of CycA2-eYFP after addition of Etoposide (Fig 6D). This suggests
331 that p21 and p53 can modulate both localisation and levels of CycA2 after DNA damage.
332
333 We detected an interaction between p21 and CycA2 in the absence of externally induced
334 DNA damage. The interaction was detected in both cytoplasmic and nuclear fractions,
335 raising the possibility that association with p21, which contains an NLS (Rodríguez-Vilarrupla
336 et al., 2002), can help translocate CycA2 to the nucleus (Fig 4C). To test whether p53 and
337 p21 contribute to the regulation of CycA2 localisation in the absence of DNA damage, we
338 next used CRISPR/Cas9 to establish p21 or p53 deficient RPE cell lines (Fig. S3B). We fixed

339 $p21^{-/-}$, $p53^{-/-}$, and WT RPE cells after a short pulse with EdU, stained using DAPI and
340 antibodies against CycA2, and quantified the levels of nuclear and cytoplasmic CycA2 in S or
341 G2-phase (Fig 6E). We observed that both $p21^{-/-}$ and $p53^{-/-}$ cell lines accumulated nuclear
342 CycA2 similar to the parental cell line. However, quantification of cytoplasmic CycA2
343 revealed that p21 deficient cells showed an increase in cytoplasmic CycA2, most apparent in
344 G2-phase. To a lower extent, we also detect increased cytoplasmic CycA2 staining in $p53^{-/-}$
345 G2 cells, but not in S-phase cells (Fig 6E). Taken together, our data indicate that p21
346 contributes to keep CycA2 nuclear, but does not support that p21 is a determining factor
347 behind the appearance of cytoplasmic CycA2 at the S/G2 transition. However, as p21 levels
348 increase after activation of a DNA damage response, p21 efficiently inhibits cytoplasmic
349 localisation of CycA2.

350 **Discussion**

351 The S/G2 transition is marked by an increase in CDK1 and PLK1 activities, which through
352 multiple feedback loops slowly build up until enforcing mitotic entry (Akopyan et al., 2014;
353 Crncec and Hochegger, 2019). How to separate the hen from the egg and identify a starting
354 point in these feedback loops has remained an unsolved question, but several studies have
355 suggested a role for CycA2 as an initiating activity (Fung et al., 2007; Gong et al., 2007; De
356 Boer et al., 2008; Mitra and Enders, 2004; Gheghiani et al., 2017; Vigneron et al., 2018).
357 However, CycA2-CDK2 activity is already present during S-phase, raising the question why
358 PLK1 activation is detected only after completion of DNA replication. One part of the answer
359 is that DNA replication activates ATR-CHK1, which restrict mitotic kinases. However,
360 inhibition of ATR-CHK1 does not cause immediate activation of PLK1 in all S-phase cells,
361 suggesting that other mechanisms contribute to restrict PLK1 activation until completion of
362 S-phase (Lemmens et al., 2018). Interestingly, whereas proteins as PLK1 and CycB1-CDK1 are
363 both nuclear and cytoplasmic, Bora – a node in the feedback loops coupling Aurora A, CDK,
364 and PLK1 – appears exclusively cytoplasmic (Feine et al., 2014; Bruinsma et al., 2015).
365

366 Here we show that CycA2 appears in the cytoplasm at the S/G2 transition. We propose a
367 model in which the rising cytoplasmic activity of CycA2-CDK initiates activation of PLK1
368 through phosphorylation of the cytoplasmic cofactor Bora (Fig 7). Later in G2, combined
369 activities of CycA2-CDK and CycB-CDK1 can further increase activation of PLK1 through
370 massive modification of Bora, eventually resulting in commitment to mitosis and protection
371 of Bora from SCF-dependent degradation (Gheghiani et al., 2017; Thomas et al., 2016; Feine
372 et al., 2014; Vigneron et al., 2018; Tavernier et al., 2015). We find no evidence that CDK1 or
373 PLK1 activities influence CycA2 localisation, supporting the idea that rather than a
374 component of feedback loops, CycA2 appearance in the cytoplasm functions as a trigger for
375 mitotic kinase activation. A parallel nuclear pathway for CDK-mediated activation of PLK1 by
376 WAC has been described (Qi et al., 2018). It remains unclear how nuclear activation of PLK1
377 fits with our observation that cytoplasmic but not nuclear CycA2 associates with PLK1, and
378 the observation that PLK1 restricted to the nucleus is not activated (Bruinsma et al., 2015).
379 One alternative can be that after initial activation mediated through Bora in the cytoplasm,
380 additional mechanisms promote PLK1 activation at later stages in G2-phase. Nonetheless,
381 PLK1 contains an NLS, which at least in *Drosophila* is exposed upon activation, allowing re-
382 distribution of active PLK1 in the cell (Kachaner et al., 2017; Taniguchi et al., 2002).
383

384 The main mechanism that regulates CycA2 cytoplasmic appearance at the S/G2 transition
385 remains unclear, although we have identified contributing factors. First, CycA2 can associate
386 with replicating chromatin, which can assist in keeping CycA2 nuclear during S-phase. The
387 restriction to the nucleus continues at least to some level during G2-phase, and we find that
388 a main player in this process is the stochiometric Cyclin/CDK interactor p21. A basal level of
389 p21 expression occurs independently of p53 in the absence of induced DNA damage,
390 although p21 levels in S-phase are generally low due to DNA-replication dependent
391 degradation (Nishitani et al., 2008; Macleod et al., 1995; Kim et al., 2008). The basal level of
392 p21 can be enhanced in a p53-dependent manner, which can restrict cytoplasmic
393 appearance of CycA2 in case of replication errors or other cellular stresses. Experimental
394 interference with the cell cycle can cause stress and p53 induction, for example as a
395 consequence of mitotic delay (Uetake and Sluder, 2010). Caution is therefore required when
396 interpreting results after cell cycle perturbation, such as depletion of CDK1.
397
398 The levels of CycA2 increase dramatically from early S-phase to late G2-phase. An attractive
399 but speculative model would be that DNA replication and non-DNA replication-dependent
400 interactions keep an amount of Cyclin A2 sequestered in the nucleus. This raises the
401 possibility that increasing CycA2 levels through G2-phase could eventually surpass the
402 amount of CycA2 sequestered in the nucleus and appear in the cytoplasm. How additional
403 mechanisms behind CycA2 cytoplasmic appearance that are not identified in this study fit
404 into the model remains unclear (Fig 7).
405
406 A long standing idea in the cell cycle field has been that upon stress, cell cycle progression
407 can be delayed by altering the localisation of key proteins as Cdc25B, Cdc25C, and CycB1
408 (Takizawa and Morgan, 2000). We and others previously showed that upon DNA damage,
409 terminal cell cycle exit from G2-phase is marked by a p21-dependent abrupt translocation of
410 CycB1 to the nucleus, followed by APC/C-dependent degradation (Mullers et al., 2014;
411 Krenning et al., 2014; Johmura et al., 2014). Here we find that with respect to pattern of
412 expression, localisation changes, and timings, CycA2 behaves similar to CycB1 after DNA
413 damage in G2-phase. It is tempting to speculate that CycA2 nuclear restriction after DNA
414 damage prevents PLK1 activation in the cytoplasm while allowing nuclear functions such as
415 stimulating transcription of p21 (Müllers et al., 2017). This opens up the possibility that
416 CycA2 not only is upstream in activating mitotic kinases, but also for triggering cell cycle exit
417 from G2-phase in case of excessive DNA damage.

418

419 The regulated appearance of CycA2 in the cytoplasm at the S/G2 transition suggests that
420 CycA2 can direct CDK activity both in a temporal and spatial manner. This is similar to CycB1,
421 whose change in localisation prior to mitosis provides access to nuclear substrates (Pines
422 and Hunter, 1991). Given that multiple cytoplasmic targets of CycA2 have been described,
423 and that CDK2 is identified as a major interaction hub in the cytoskeleton, we note the
424 possibility that apart from PLK1 activation, various processes are differentially regulated
425 before and after completion of S-phase. (Kanakkanthara et al., 2016; Woodman et al., 1993;
426 Arsic et al., 2012; Tsang et al., 2007; Thul et al., 2017)

427

428 **Acknowledgements**

429 We thank the members of Lindqvist and Macurek labs for comments and suggestions, and
430 Patrick von Morgen for technical assistance. This work was supported by grants from the
431 Swedish Research Council, the Swedish Foundation for Strategic Research, the Swedish
432 Cancer Society and the Czech Science Foundation (17-04742S).

433

434 **Author contributions**

435 Conceptualization: HSC, EM, AL
436 Funding acquisition: LM, AL
437 Investigation: All authors
438 Supervision: LB, LM, AL
439 Writing – original draft: HSC, AL
440 Writing – review and editing: All authors

441

442 **Competing interests**

443 Erik Müllers is an employee of AstraZeneca. Other authors declare no competing interests.

444 ## Materials and Methods

445 **Cell culture**

446 Human hTERT-RPE1 (hereafter referred to as RPE), U2OS and HeLa cells were cultured in an
447 ambient-controlled incubator at 37°C and 5% CO_2. All cells were a kind gift from René
448 Medema and were regularly controlled for mycoplasma infection. RPE cells were cultured
449 using DMEM-F12 + GlutaMAX (Invitrogen) supplemented with 10% heat-inactivated FBS
450 (HyClone) and 1% P/S (HyClone). U2OS and HeLa cells were cultured using DMEM +
451 GlutaMAX (Invitrogen) supplemented with 6% heat-inactivated fetal bovine serum (FBS,
452 HyClone) and 1% Penicillin/Streptomycin (P/S, HyClone). For adeno-associated virus
453 production, HEK293 cells were cultured using DMEM + GlutaMAX (Invitrogen) supplemented
454 with 10% heat-inactivated fetal bovine serum (FBS, HyClone) and 1% Penicillin/Streptomycin
455 (P/S, HyClone). For live-cell imaging experiments the medium of the cells was changed to
456 Leibowitz-15 (Invitrogen) supplemented with 10% FBS (HyClone) and 1% P/S (HyClone).
457

458 **Establishment of cell lines**

459 RPE CycA2-eYFP cells were obtained by adeno-associated (AAV)-mediated homologous
460 recombination as previously described (Akopyan et al., 2014). Briefly, the targeting cassette
461 was designed to contain an arm of 1.1 kb of homology with the sequence directly 5' of the
462 *CCNA2* Stop codon followed by the ORF of EYFP and another arm of homology 1.016 kb with
463 the 3' UTR of the *CCNA2* gene. Adeno-associated viruses containing the homology cassette
464 were produced and used to transduce RPE cells. Four days after transduction cells were
465 sorted by FACS to enrich the YFP-positive population. After two rounds of sorting, single YFP
466 positive cells were seeded in 96-well plates and clones which were validated by Western
467 blot and live-cell imaging. Knock out of *TP53* and *p21* in RPE cells using CRISPR/Cas9 was
468 generated as described previously (Pechackova et al., 2016) and independent clones were
469 validated by Western blotting and sequencing of the genetic loci. For expression of CycA2
470 localisation variants, CycA2 constructs containing silent mutations to the 4 SMARTpool ON-
471 TARGET plus siRNAs targeting CycA2, linked to mCherry and coupled to NLS or NES
472 sequences as indicated in Figure 3C, and flanked by Piggy-Bac integration sites, were
473 synthesised by Vector Builder. Sequence information is available at
474 https://en.vectorbuilder.com/design/retrieve.html for vectors VB190920-1050khh and
475 VB190920-1053jda. The vectors were co-transfected into RPE $p53^{-/-}$ cells expressing Dox-
476 inducible OsTIR from the Rosa locus (Lemmens et al., 2018), with vectors for GFP flanked by

477 Piggy-Bac integration sites and Piggy-Bac transposase. After selection with Blasticidin,
478 polyclonal populations were used and only GFP positive cells were analysed.
479
480 **Cell synchronisation**
481 RPE or RPE CycA2-eYFP cells were synchronized in G0 by growing to confluency, split to fresh
482 medium supplemented with thymidine (2 mM) and grown for 40 h. Cells were released to
483 fresh medium and collected after 5h. Synchronisation efficiency was validated by flow
484 cytometry using 4n DNA content and absence of pS10-H3 staining as G2 markers. Typically,
485 this protocol yielded >95% G2 population and less than 0.5 % mitotic cells. Alternatively,
486 where indicated, RPE or RPE CycA2-eYFP cells were synchronized in S-phase by addition of
487 HU.
488
489 **Cell fractionation and Immunoprecipitation**
490 Cells were fractionated using hypotonic lysis as previously described (Andersen et al., 2002).
491 Briefly, cells were collected by trypsinization and centrifugation (300 g for 5 min at 4°C), and
492 washed with PBS. The cell pellet was resuspended in 5× packed cell volume of hypotonic
493 buffer A (10 mM HEPES-KOH, pH 7.9, 10 mM KCl, 1.5 mM $MgCl_2$, 0.5 mM DTT, and 0.5 mM
494 PMSF) supplemented with a cocktail of protease inhibitors (cOmplete, EDTA free; Roche)
495 and phosphatase inhibitors (PhosSTOP, Roche) and incubated on ice for 5 min. Next, the
496 cells were spun down at 500 g for 5 min, suspended in 2× packed cell volume of
497 supplemented buffer A and dounced using a tight-fitting pestle. Nuclei were collected by
498 centrifugation at 500 g for 5 min at 4°C. Supernatant was centrifuged 20000g 10 min 4°C,
499 supplemented with NaCl and Triton X-100 to 150 mM and 0.1 % final concentration,
500 respectively and used as cytoplasmic fraction. Nuclei were cleaned by centrifugation over
501 sucrose gradient, lysed in lysis buffer (10 mM HEPES pH 7.9, 10 mM KCl, 150 mM NaCl, 1.5
502 mM MgCl2, 0.1 % NP-40, 0.5mM DTT, 0.5 mM PMSF supplemented with protease inhibitor
503 cocktail and PhosSTOP), sonicated and cleared by centrifugation at 20000 g 10min 4°C. For
504 IP 2 mg of cytoplasmic and nuclear extracts were incubated with either 15 µl GFP Trap beads
505 (Chromotek) for 1 h at 4°C or 1-1.5 µg IgG overnight at 4°C, Protein A/G Ultralink beads were
506 added for last 2 h. Beads were washed four times with lysis buffer and precipitates were
507 eluted to SDS-PAGE sample buffer.
508 For figure 5C, Protein fractionation was performed according to (Baranello et al., 2016) with
509 minor changes. To prepare the extracts, cells were washed once with PBS and twice with
510 Hepes Wash Buffer (20 mM Hepes pH 7.5, 137 mM NaCl). After incubation with Hepes Lysis

511 buffer (10 mM HEPES pH 7.5) cell were scraped and collected, smashed through a 20 gauge
512 needle and then centrifuged for 10 min at 800g at 4ºC. Supernatant containing the
513 cytoplasmic proteins was collected and the pellet was washed with HEPES Lysis buffer,
514 centrifuged and finally resuspended in RIPA 137 buffer (50 mM Tris-HCl pH 7.5, 137 mM
515 NaCl, 1% NP-40). A 25 gauge needle was used to destroy the nuclear membranes, then the
516 sample was centrifuged at 4000 rpm for 10 min 4°C and the supernatant containing nuclear
517 soluble proteins was collected. Pellet was resuspended in RIPA 400 buffer (50 mM Tris-HCl
518 pH 7.5, 400 mM NaCl, 1% NP-40) and sonicated with Diagenode Bioruptor Sonicator for 5
519 min (low sonication setting, 30 seconds on – 30 seconds off). Samples were centrifuged at
520 12000 rpm for 10 min at 4ºC and supernatant containing chromatin bound nuclear proteins
521 collected and equilibrated to RIPA 137 buffer.
522
523 **Chromatin Immunoprecipitation (ChIP) and qPCR**
524 ChIP samples were prepared from RPE-CycA2-eYFP cells as described in (Baranello et al.,
525 2016) with minor changes. Briefly $8x10^6$ cells were crosslinked with 1% formaldehyde for 5
526 min. Cross-linking was stopped by the addition of glycine to 125 mM final concentration and
527 cells were washed twice with cold PBS. After harvesting cells by scraping, the pellet was
528 washed once with PBS plus 0.5% BSA and resuspended in TE-SDS 0.1% (10 mM Tris-HCl pH
529 8.0, 1 mM EDTA pH 8.0, SDS 0.1%) supplemented with complete protease inhibitor tablet
530 (Roche) to a final concentration of $4.5x10^6$ cells/ml. Samples were sonicated for 20 min with
531 Covaris ME220 sonicator using the 1ml High Cell protocol (Peak power: 75, Duty % factor:
532 15, Cycles/Burst: 1000, Average power: 11.25) to produce chromatin fragments of 400 bp on
533 average. After clarification by centrifugation, sonicated extracts were adjusted to the
534 conditions of RIPA buffer (10mM Tris pH 8.0, 1mM EDTA pH 8.0, 1% Triton X-100, 0.1% SDS,
535 200mM NaCl, Na Deoxycholate 0.1%).
536 3 µg of anti-GFP (ab290) or IgG (sc2025) were mixed with 40 µl of Dynabeads Protein A
537 (Invitrogen) and incubated at 4°C for 6 h with rotation. Chromatin from 8×10^6 cells was
538 added to the Protein A-antibody complexes and incubated overnight at 4°C with rotation.
539 Immunoprecipitates were washed twice with RIPA buffer (10 mM Tris-HCl pH 8.0, 1 mM
540 EDTA pH 8.0, 1% Triton X100, 0.1% Na-Deoxycholate, 0.1% SDS, 200 mM NaCl); twice with
541 RIPA buffer plus 300 mM NaCl; once with LiCl buffer (10 mM Tris-HCl pH 8.0, 1 mM EDTA pH
542 8.0, 250 mM LiCl, 0.5% NP40, 0.5% Na-Deoxycholate); and twice with TE. The beads were
543 then resuspended in 100 µl TE plus 0.25% SDS supplemented with proteinase K (500 µg/ml,
544 Roche) and incubated overnight at 60°C. The DNA was recovered from the eluate by phenol

545 chloroform extraction followed by ethanol precipitation in the presence of 20 µg of
546 GlycoBlue (Invitrogen) and dissolved in TE. qPCR was performed using the 7500 Fast Real-
547 Time PCR system (Applied Biosystem) and Fast SYBR Green Master Mix (Thermo Fisher
548 Scientific). 7500 Software (Applied Biosystem) was used for quantification by standard curve
549 method and data was plotted as percentage of input, ratio of the signal from
550 immunoprecipitated DNA to the signal of input DNA. Five genomic locations were analyzed.
551 The detection primers are listed in Supplementary Table 1.
552
553 **Inhibitors**
554 For live-cell imaging and quantitative immunofluorescence experiments, the following
555 inhibitors were used at the indicated concentrations for 4 h unless indicated differently in
556 the experiments: RO-3306 at 10 µM (CDK1 inhibitor; Calbiochem), NU6140 at 10 µM (CDK2
557 inhibitor; Calbiochem), MK-1775 at 5 µM (Wee1 inhibitor; Selleck Chemicals), Etoposide
558 2µM (topoisomerase II inhibitor; Sigma Aldrich), Neocarzinostatin at 2 nM (radiomimetic
559 drug; Sigma Aldrich), Thymidine at 2.5 mM (Sigma Aldrich) and Hydroxyurea at 2 mM
560 (ribonucleotide reductase inhibitor; Sigma Aldrich).
561
562 **siRNA transfection**
563 SMARTpool ON-TARGET plus siRNAs targeting CycA2, CDK1, CDK2, p21 or p53 as well as a
564 scrambled control siRNA were purchased from Dharmacon and employed at a concentration
565 of 20nM using HiPerFect transfection reagent (Qiagen) and OptiMEM (Invitrogen) at 48h and
566 24h before live-cell imaging or fixation.
567
568 **Live-cell microscopy**
569 For live cell imaging, cells were seeded in 96-well imaging plates (BD Falcon) using Leibowitz-
570 15 medium (Invitrogen) and followed on an ImageXpress system (Molecular Devices) using a
571 20x NA 0.45 objective or on a Leica DMI6000 Imaging System using a 20x NA 0.4 objective.
572 Images were processed and analysed using ImageJ. Nuclei and cytoplasm were selected by
573 manual drawing. FRET microscopy was performed as in (Hukasova et al., 2012) and
574 simultaneous monitoring of FRET and a PCNA chromobody was performed as in (Akopyan et
575 al., 2014).
576
577 **FRAP**

578 FRAP microscopy on RPE CycA2-eYFP was performed on a Zeiss LSM710 microscope, using a
579 40X/NA1,2 objective and a 514 nm laser. Fluorescence intensities of two 10x50 pixel regions
580 in the same nucleus were recorded at 44 images/second. Bleaching was performed in one
581 region with 100% laser power for 1.5 seconds after acquiring 200 images. After background
582 subtraction, estimated from an area next to the cell before scanning, the ratio between the
583 bleached and unbleached region in the same nucleus was calculated over time.
584
585 **Antibodies**
586 The following antibodies were used: GFP (ab13970 abcam), GFP (ChIP; ab290) Cyc A2 (#sc-
587 751, Santa Cruz) (used for immunofluorescence), CycA2 (#4656 Cell Signalling), CycA2
588 (HPA020626), PLK1 (ab14210; Abcam), affinity purified mouse anti pT210-PLK1 (clone K50-
589 483, Becton Dickinson), affinity purified rabbit anti-Bora (Bruinsma et al., 2014), CDK1 (sc-
590 54, Santa Cruz and #9116 Cell Signalling), CDK2 (sc-163, Santa Cruz and #2564 Cell
591 Signalling), GAPDH (G9545 Sigma Aldrich), H2B (ab1790 abcam), β-Tubulin (#2128S Cell
592 Signalling), PCNA (HPA030522), KAP1 (A300-274A), H3 (ab1791), Alexa Fluor 488-Goat anti-
593 chicken (#A11039 Life Technologies) and Alexa Fluor 647-Donkey anti-rabbit (#A31537 Life
594 Technologies).
595
596 **Quantitative immunofluorescence**
597 For quantitative immunofluorescence experiments 10.000 cells were seeded 16h before the
598 different treatments with inhibitors. For siRNA transfections, 5.000 cells were seeded
599 instead. Twenty min before fixation EdU (5-ethynyl-2'-deoxyuridine, Molecular probes) was
600 added in all the experiments. Cells were fixed using 3.7% formaldehyde (Sigma Aldrich) for 5
601 min and permeabilised using -20°C methanol (Sigma Aldrich) for 2 minutes, blocking was
602 performed using 2% bovine albumin serum (BSA; Sigma Aldrich) in TBS supplemented with
603 0.1% Tween20 (TBS-T). After blocking, cells were incubated with primary antibodies at 4°C
604 overnight. After washing, cells were incubated with secondary antibodies and DAPI for 1h at
605 room temperature. Click chemistry was performed after wash of the secondary antibody
606 using a mixture of 100mM Tris, 1mM $CuSO_4$, 100mM ascorbic acid and fluorescent dye
607 (#A10277 and #A10266, Invitrogen) and incubated for 1h at room temperature. Images were
608 acquired on an ImageXpress system (Molecular Devices) using either a 20x (NA) objective or
609 a 40x NA 0.6 objective. Images were manually screened and processed and analysed using
610 CellProfiler (Carpenter et al., 2006) to identify and measure nuclear and cytoplasmic
611 fluorescence intensity of single cells. Cell cycle stages were determined setting a threshold

612 both on DAPI and EdU levels. For time-estimates based on fixed cells, CycA2 and DAPI
613 measurements were corrected using a background function and 2-4N DNA content cells
614 were sorted based on the 90th percentile CycA2 and DAPI measurement, as described in
615 (Akopyan et al., 2016).
616
617 ***In vitro* kinase assay**
618 Kinase dead PLK1-K82R, GST-Bora and GST-Aurora-A were purified from bacteria as
619 described (Macurek et al., 2008) and incubated with CycA2-CDK2 (100 ng/reaction, Biaffin
620 GmbH) in a kinase buffer (25 mM MOPS pH 7.2, 12.5 mM glycerol 2-phosphate, 25 mM
621 MgCl2, 5 mM EGTA, 2 mM EDTA and 0.25 mM DTT) supplemented with 100 μM ATP and 5
622 μCi 32P-γ-ATP at 30°C for 30 min. After separation of proteins by SDS-PAGE, phosphorylation
623 was detected by autoradiography or by pT210-PLK1 antibody.
624
625 **Data availability**
626 Data generated or analysed during this study are included in this published article or
627 available upon request.

628 ## Figure legends

629 **Figure 1. Cyclin A2 accumulates in the cytoplasm at the S/G2 transition**

630 (**a**) Time-lapse imaging through mitosis of a single RPE cell gene-targeted to express CycA2-
631 eYFP. Time between images is 20 minutes.

632 (**b**) Quantification of mean fluorescence intensity in the nucleus (top) and in the cytoplasm
633 (middle) of 50 individual RPE CycA2-eYFP cells over time. Cells were synchronised *in silico* to
634 set t=0 at mitosis. Nuclear and cytoplasmic fluorescence in mitosis is approximated to
635 central and peripheral regions of the mitotic cell in order to show a continuous graph. Please
636 note that the increase in mean intensity during mitosis largely is due to cell rounding.
637 Bottom graph shows the average of nuclear and cytoplasmic mean intensities.

638 **(c)** Time-course estimate from fixed cells, pulse-labelled with EdU. 2100 RPE-CycA2-eYFP
639 cells were sorted based on increasing anti-GFP and DAPI staining (left) and 1567 RPE cells
640 were sorted based on increasing anti-CycA2 and DAPI staining (right). Graphs focus on area
641 where CycA2 expression is apparent. Lower graphs show running median of 100 (left) or 50
642 (right) cells.

643 (**d**) Western blot of nuclear and cytoplasmic fractions of unsynchronised RPE-CycA2-eYFP
644 cells using the indicated antibodies.

645 (**e**) Quantification of the percentage of cells accumulating CycA2-eYFP in the cytoplasm after
646 different treatments. Cells were treated with DMSO (Control), Thymidine or Hydroxyurea
647 and imaged. The number of cells accumulating CycA2 in the cytoplasm was recorded and
648 plotted as a percentage of the total number of cells tracked.

649 All experiments were repeated at least three times.

650

651 **Figure 2. CycA2 containing nuclear export sequences can rescue cell cycle arrest after**
652 **depletion of endogenous CycA2**

653 **(a)** Time-lapse sequence of U2OS cells expressing PLK1 FRET reporter and PCNA
654 chromobody. Time points (h) are indicated in figure. Top Ctrl siRNA, bottom CycA2 siRNA.

655 **(b)** Quantification of individual cells, imaged as in (a). Red line shows 1/FRET and blue line
656 shows PCNA foci.

657 **(c)** Schematic of siRNA-non-targetable CycA2 expression constructs.

658 **(d)** Images show RPE p53$^{-/-}$ TetON OsTIR, cotransfected with Piggy-BAC transposase, GFP
659 flanked by Piggy-BAC integration sites (to mark transfected cells) and the constructs outlined
660 in (c) after 18h Doxycycline addition.

661 **(e)** Quantification of mitotic entry in GFP-expressing cells. Polyclonal populations as in (d)
662 were transfected with CycA2 siRNA. 48h later, cells were transferred to L15 medium with or
663 without Doxycycline and followed by time-lapse microscopy. At least 275 cells were followed
664 per condition.
665
666 **Figure 3. Cytoplasmic CycA2 triggers PLK1 activation.**
667 **(a)** Inhibition of CDK activity in U2OS cells expressing PLK1 FRET reporter. Cells with
668 intermediate PLK1 FRET signal, indicative of G2-phase, were followed after addition of
669 indicated inhibitors. Graph shows average and s.e.m of at least 10 cells per condition.
670 **(b)** Inhibition of CDK activity in RPE cells synchronised in G2 decreases the level of PLK1
671 phosphorylation at T210.
672 **(c)** Phosphorylation of Bora by CycA2-CDK2 promotes modification of PLK1 at T210 mediated
673 by Aurora-A. Empty arrowhead indicates position of the kinase dead PLK1, full arrowhead
674 indicates position of Bora.
675 **(d)** CycA2-CDK2 can phosphorylate Bora on SP/TP sites**.**
676 **(e, f)** Cytosolic and nuclear extracts from RPE cells synchronised in G2-phase were subjected
677 to immunoprecipitation with anti-CycA2 (e) or anti-PLK1 (f) antibodies and bound proteins
678 were probed with indicated antibodies.
679 **(g)** Expression of PLK1 T210D can partially rescue CycA2 siRNA-mediated cell cycle arrest.
680 U2TR cells with inducible expression of PLK1 T210D were transfected with CycA2 siRNA. 20h
681 later, Doxycycline was added and cells were followed using phase contrast time-lapse
682 microscopy. 300 cells per condition were followed manually over time.
683 All experiments were repeated at least three times.
684
685 **Figure 4. CDK1 can contribute to cytoplasmic accumulation of Cyclin A2**
686 **(a)** Cells were transfected with siRNAs for either CDK1 or CDK2 for 48 h, incubated with EdU
687 for 20 min and fixed. Arrows indicate G2 cells with low cytoplasmic CycA2.
688 **(b)** Quantification of cytoplasmic and nuclear integrated intensities of CycA2 in at least 500
689 RPE cells imaged as in (a). Cells were gated for DAPI and EdU levels and assigned to S-phase
690 (red dots) or G2-phase (green dots). Each dot represents one cell; the percentages indicate
691 the proportion of S- and G2-phase cells in each condition. Number of cells within indicated
692 gate and total amount of G2 cells are shown to the right.
693 **(c)** RPE (RPE) or RPE CycA2-eYFP (CycA2) cells were synchronised in G2, separated to
694 cytosolic and nuclear fractions and immunoprecipitated with GFP Trap (left) or with control

695 IgG and CycA2 antibody (right). Proteins bound to the carrier were probed with indicated
696 antibodies. All experiments were repeated at least three times.
697
698 **Figure 5. Cyclin A2 associates with chromatin during S-phase.**
699 (**a**) Chromatin immunoprecipitation (ChIP) in RPE-CycA2-eYFP cells, synchronized with
700 hydroxyurea (HU, 2mM in PBS) for 18 h and harvested after HU washout at different
701 timepoints (0, 4 and 8 h). The enrichment of CycA2-eYFP and IgG, determined by ChIP-qPCR
702 is plotted as percentage of input (ratio of immunoprecipitated DNA to the total amount of
703 DNA). Genomic locations are indicated by alphabetical letters A-E, (details in supplementary
704 Table1). Graph shows one representative experiment. Mean value and SD are based on
705 duplicate samples, each with duplicate qPCR reactions. Mean relative recovery for non-
706 immune IgG are 0.0072. Asterisks indicate two-tailed paired Student's t test; *P < 0.05, **P <
707 0.01, ***P < 0.001, ****P < 0.0001.
708 (**b**) Fluorescence recovery after photobleaching (FRAP) in the nucleus of RPE-CycA2-eYFP
709 cells. Graph shows normalised average of cells with (G2-phase) and without (S-phase)
710 detectable cytoplasmic CycA2-eYFP. N=2.
711 (**c**) RPE-CycA2-eYFP cells were synchronised with hydroxyurea for 18 h and harvested after 4
712 and 10 h in HU-free media. Cytoplasmic proteins (Cyto), soluble nuclear proteins (N.sol) and
713 chromatin bound proteins (Chr) were isolated and detection of Cyclin A2 and PCNA was
714 performed by Western blot. 5 μg of protein was loaded for each fraction. β-Tubulin, KAP1
715 and Histone H3 were used as controls of cytosolic, nuclear soluble and chromatin fraction,
716 respectively. N=2.
717
718 **Figure 6. p21 can modulate cytoplasmic accumulation of Cyclin A2-eYFP**
719 **(a)** Time-lapse images of RPE CycA2-eYFP cell treated with 2 nM Neocarzinostatin (NCS).
720 Asterisk indicates a cell exposed to NCS in S-phase, and arrow indicates a cell exposed to
721 NCS in G2-phase.
722 **(b)** Quantification of average nuclear and cytoplasmic CycA2-eYFP intensity after NCS
723 addition. RPE CycA2-eYFP cells were imaged as in (a). Graphs show quantification over time
724 in single cells, separated in cells showing cytoplasmic CycA2-eYFP at time of NCS addition
725 (left, G2-phase, n=10) or not (right, S-phase, n=10). No cell entered mitosis.
726 **(c)** Quantification of average nuclear and cytoplasmic CycA2-eYFP intensity after Etoposide
727 and MG132 addition. RPE CycA2-eYFP cells that showed both nuclear and cytoplasmic
728 fluorescence (G2 cells) at start of experiment were followed over time. Graphs show

729 quantification over time in single cells, separated in cells entering mitosis before Etoposide
730 addition (left, n=9, plotted until time-point before mitosis), Etoposide addition alone
731 (middle, n=8), Etoposide and MG132 addition (n=9).
732 **(d)** RPE CycA2-eYFP cells were transfected with p21, p53 or control siRNAs for 48 h and
733 treated with Etoposide at t=0. Single cells were tracked over time and the time point of loss
734 of CycA2-eYFP was determined visually. Graph shows cytoplasmic and nuclear loss of CycA2-
735 eYFP of at least 100 cells that contained cytoplasmic CycA2-eYFP at time point of addition of
736 Etoposide addition.
737 **(e)** WT (ctrl), $p21^{-/-}$ or $p53^{-/-}$ RPE cells were incubated for 20 min with EdU and fixed. Graph
738 to left shows quantification of integrated intensity of EdU staining versus nuclear DAPI
739 intensity in at least 1500 wt cells; each circle represents one cell. The large grey rectangle
740 indicates gating for EdU positive cells (S-phase) and the small grey rectangle indicates gating
741 for EdU-negative 4N cells (G2). Box plots to right show 90, 75, 50, 25, and 10 percentiles of
742 cells in S-phase (top) and in G2-phase (bottom). Squares indicate average value. * indicates
743 $p<0.05$, *** indicates $p<0.0001$, Student's t-test.
744
745 **Figure 7. A model for PLK1 activation by cytoplasmic CycA2.**
746 CycA2 is restricted to the nucleus during S-phase. At the S/G2 transition, part of CycA2
747 localises to the cytoplasm, where it can phosphorylate Bora, resulting in activation of PLK1.
748

749 ## Supplementary figure legends

750 **Supplementary figure 1. Validation of Cyclin A2-eYFP cell lines**
751 **(a)** Western blot of cell lines indicated. GAPDH is used as loading control.
752 **(b)** Time-lapse images of U2OS CycA2-eYFP cells. Time between images is 20 min.
753 **(c)** RPE CycA2-eYFP cells were incubated for 20 min with EdU and fixed. Left graphs shows
754 quantification of nuclear and cytoplasmic integrated intensity of GFP staining versus nuclear
755 DAPI intensity in at least 1500 cells; each dot represents one cell. Middle graph shows
756 nuclear versus cytoplasmic integrated intensities of GFP staining; the grey square indicates
757 the gating for expressors of both nuclear and cytoplasmic CycA2-eYFP. Right graphs show
758 integrated EdU intensity versus integrated DAPI intensity, with or without gating for
759 expressors of both nuclear and cytoplasmic CycA2-eYFP (bottom right).
760 **(d)** RPE cells were treated as in (c), and stained with CycA2 antibodies. At least 1200 cells
761 were quantified.
762

763 **Supplementary figure 2. Cyclin A2-eYFP cytoplasmic appearance after modulation of CDK**
764 **activity**
765 (**a**) Quantification of nuclear (left) and cytoplasmic (right) accumulation of CycA2-eYFP in at
766 least 17 single cells treated with DMSO (top), RO-3306 (middle) or Nu6140 (bottom) for 4 h;
767 each track represents a single cell. Cells were selected based on clear but low cytoplasmic
768 CycA2-eYFP signal at time point of inhibitor addition, and synchronised *in silico* at the time
769 point when cells reached a threshold of cytoplasmic CycA2-eYFP (indicated with the grey
770 dotted line). (Below) Average intensities. Error bars show SD. Please note that differences
771 after 2h involve that DMSO treated cells enter mitosis, giving an increase in average
772 fluorescence upon cell rounding followed by a drop in fluorescence upon mitotic CycA2-eYFP
773 degradation.
774 (**b**) Quantification of at least 95 single RPE-CycA2-eYFP cells upon treatment with either
775 DMSO (control) or Wee1 inhibitor (MK1775). Cells were treated with the drugs and tracked
776 using live-cell imaging. Each track represents one single cell, the black dot represents the
777 first time point when cytoplasmic CycA2 can be detected and the red dot indicates mitotic
778 entry. Overlap of the cumulative appearance of cytoplasmic CycA2 in the two different
779 treatments (right).
780 **(c)** Western blot of cells transfected with CDK1, CDK2 or scrambled (Control) siRNAs for 48 h.
781 Samples were prepared from 4 wells in a 96-well plate to mimic conditions used for
782 microscopy.
783 **(d)** Proportion of cells passing through mitosis during 16 h after knock down of CDK1 or
784 CDK2 for 48 h (left). Duration of mitosis in the indicated knockdown conditions (right).
785
786 **Supplementary figure 3. Validation of p21$^{-/-}$ and p53$^{-/-}$ cell lines**
787 **(a)** Time-lapse microscopy of a G2-phase RPE CycA2-eYFP cell after Etoposide addition.
788 **(b)** Western blot of indicated cell lines (two different clones of p21$^{-/-}$ and p53$^{-/-}$ RPE cell
789 lines). KAP1 and TFIIH are used as loading controls.
790
791 **Supplementary Table 1**
792 List of primers used for qPCR

793 **References**

794 Abdurashidova, G., M. Deganuto, R. Klima, S. Riva, G. Biamonti, M. Giacca, and A.
795 Falaschi. 2000. Start sites of bidirectional DNA synthesis at the human lamin
796 B2 origin. *Science*. 287:2023–2026. doi:10.1126/science.287.5460.2023.

797 Akopyan, K., A. Lindqvist, and E. Mullers. 2016. Cell Cycle Dynamics of Proteins and
798 Post-translational Modifications Using Quantitative Immunofluorescence.
799 *Methods Mol Biol*. 1342:173–83. doi:10.1007/978-1-4939-2957-3_9.

800 Akopyan, K., H. Silva Cascales, E. Hukasova, A.T. Saurin, E. Mullers, H. Jaiswal, D.A.
801 Hollman, G.J. Kops, R.H. Medema, and A. Lindqvist. 2014. Assessing kinetics
802 from fixed cells reveals activation of the mitotic entry network at the S/G2
803 transition. *Mol Cell*. 53:843–53. doi:10.1016/j.molcel.2014.01.031.

804 Andersen, J.S., C.E. Lyon, A.H. Fox, A.K.L. Leung, Y.W. Lam, H. Steen, M. Mann, and
805 A.I. Lamond. 2002. Directed proteomic analysis of the human nucleolus. *Curr.*
806 *Biol. CB*. 12:1–11. doi:10.1016/s0960-9822(01)00650-9.

807 Arsic, N., N. Bendris, M. Peter, C. Begon-Pescia, C. Rebouissou, G. Gadea, N.
808 Bouquier, F. Bibeau, B. Lemmers, and J.M. Blanchard. 2012. A novel function
809 for Cyclin A2: control of cell invasion via RhoA signaling. *J Cell Biol*. 196:147–
810 62. doi:10.1083/jcb.201102085.

811 Baranello, L., D. Wojtowicz, K. Cui, B.N. Devaiah, H.-J. Chung, K.Y. Chan-Salis, R.
812 Guha, K. Wilson, X. Zhang, H. Zhang, J. Piotrowski, C.J. Thomas, D.S. Singer,
813 B.F. Pugh, Y. Pommier, T.M. Przytycka, F. Kouzine, B.A. Lewis, K. Zhao, and D.
814 Levens. 2016. RNA Polymerase II Regulates Topoisomerase 1 Activity to Favor
815 Efficient Transcription. *Cell*. 165:357–371. doi:10.1016/j.cell.2016.02.036.

816 Bendris, N., B. Lemmers, J.-M. Blanchard, and N. Arsic. 2011. Cyclin A2 mutagenesis
817 analysis: a new insight into CDK activation and cellular localization
818 requirements. *PloS One*. 6:e22879. doi:10.1371/journal.pone.0022879.

819 Bruinsma, W., M. Aprelia, J. Kool, L. Macurek, A. Lindqvist, and R.H. Medema. 2015.
820 Spatial Separation of Plk1 Phosphorylation and Activity. *Front. Oncol.* 5:132.
821 doi:10.3389/fonc.2015.00132.

822 Bruinsma, W., L. Macurek, R. Freire, A. Lindqvist, and R.H. Medema. 2014. Bora and
823 Aurora-A continue to activate Plk1 in mitosis. *J. Cell Sci.* 127:801–811.
824 doi:10.1242/jcs.137216.

825 Cardoso, M.C., H. Leonhardt, and B. Nadal-Ginard. 1993. Reversal of terminal
826 differentiation and control of DNA replication: cyclin A and Cdk2 specifically
827 localize at subnuclear sites of DNA replication. *Cell*. 74:979–92.

828 Carpenter, A.E., T.R. Jones, M.R. Lamprecht, C. Clarke, I.H. Kang, O. Friman, D.A.
829 Guertin, J.H. Chang, R.A. Lindquist, J. Moffat, P. Golland, and D.M. Sabatini.

830 2006. CellProfiler: image analysis software for identifying and quantifying cell
831 phenotypes. *Genome Biol.* 7:R100. doi:10.1186/gb-2006-7-10-r100.

832 Crncec, A., and H. Hochegger. 2019. Triggering mitosis. *FEBS Lett.* 593:2868–2888.
833 doi:10.1002/1873-3468.13635.

834 De Boer, L., V. Oakes, H. Beamish, N. Giles, F. Stevens, M. Somodevilla-Torres, C.
835 Desouza, and B. Gabrielli. 2008. Cyclin A/cdk2 coordinates centrosomal and
836 nuclear mitotic events. *Oncogene*. 27:4261–8. doi:10.1038/onc.2008.74.

837 Feine, O., E. Hukasova, W. Bruinsma, R. Freire, A. Fainsod, J. Gannon, H.M.
838 Mahbubani, A. Lindqvist, and M. Brandeis. 2014. Phosphorylation-mediated
839 stabilization of Bora in mitosis coordinates Plx1/Plk1 and Cdk1 oscillations.
840 *Cell Cycle Georget. Tex*. 13:1727–1736. doi:10.4161/cc.28630.

841 Frouin, I., M. Toueille, E. Ferrari, I. Shevelev, and U. Hubscher. 2005. Phosphorylation
842 of human DNA polymerase lambda by the cyclin-dependent kinase
843 Cdk2/cyclin A complex is modulated by its association with proliferating cell
844 nuclear antigen. *Nucleic Acids Res*. 33:5354–61. doi:10.1093/nar/gki845.

845 Fung, T.K., H.T. Ma, and R.Y. Poon. 2007. Specialized roles of the two mitotic cyclins
846 in somatic cells: cyclin A as an activator of M phase-promoting factor. *Mol*
847 *Biol Cell*. 18:1861–73. doi:10.1091/mbc.E06-12-1092.

848 Furuno, N., N. den Elzen, and J. Pines. 1999. Human cyclin A is required for mitosis
849 until mid prophase. *J Cell Biol*. 147:295–306.

850 Gheghiani, L., D. Loew, B. Lombard, J. Mansfeld, and O. Gavet. 2017. PLK1 Activation
851 in Late G2 Sets Up Commitment to Mitosis. *Cell Rep.* 19:2060–2073.
852 doi:10.1016/j.celrep.2017.05.031.

853 Gong, D., and J.E. Ferrell Jr. 2010. The roles of cyclin A2, B1, and B2 in early and late
854 mitotic events. *Mol Biol Cell*. 21:3149–61. doi:10.1091/mbc.E10-05-0393.

855 Gong, D., J.R. Pomerening, J.W. Myers, C. Gustavsson, J.T. Jones, A.T. Hahn, T.
856 Meyer, and J.E. Ferrell Jr. 2007. Cyclin A2 regulates nuclear-envelope
857 breakdown and the nuclear accumulation of cyclin B1. *Curr Biol*. 17:85–91.
858 doi:10.1016/j.cub.2006.11.066.

859 Hégarat, N., A. Crncec, M.F. Suarez Peredo Rodriguez, F. Echegaray Iturra, Y. Gu, O.
860 Busby, P.F. Lang, A.R. Barr, C. Bakal, M.T. Kanemaki, A.I. Lamond, B. Novak, T.
861 Ly, and H. Hochegger. 2020. Cyclin A triggers Mitosis either via the Greatwall
862 kinase pathway or Cyclin B. *EMBO J.* e104419.
863 doi:10.15252/embj.2020104419.

864 Hein, J.B., and J. Nilsson. 2016. Interphase APC/C-Cdc20 inhibition by cyclin A2-Cdk2
865 ensures efficient mitotic entry. *Nat Commun*. 7:10975.
866 doi:10.1038/ncomms10975.

867 Hukasova, E., H. Silva Cascales, S.R. Kumar, and A. Lindqvist. 2012. Monitoring kinase
868 and phosphatase activities through the cell cycle by ratiometric FRET. *J. Vis.*
869 *Exp. JoVE*. e3410. doi:10.3791/3410.

870 Jackman, M., Y. Kubota, N. den Elzen, A. Hagting, and J. Pines. 2002. Cyclin A- and
871 cyclin E-Cdk complexes shuttle between the nucleus and the cytoplasm. *Mol*
872 *Biol Cell*. 13:1030–45. doi:10.1091/mbc.01-07-0361.

873 Johmura, Y., M. Shimada, T. Misaki, A. Naiki-Ito, H. Miyoshi, N. Motoyama, N. Ohtani,
874 E. Hara, M. Nakamura, A. Morita, S. Takahashi, and M. Nakanishi. 2014.
875 Necessary and sufficient role for a mitosis skip in senescence induction. *Mol.*
876 *Cell*. 55:73–84. doi:10.1016/j.molcel.2014.05.003.

877 Kachaner, D., D. Garrido, H. Mehsen, K. Normandin, H. Lavoie, and V. Archambault.
878 2017. Coupling of Polo kinase activation to nuclear localization by a
879 bifunctional NLS is required during mitotic entry. *Nat. Commun.* 8:1701.
880 doi:10.1038/s41467-017-01876-8.

881 Kanakkanthara, A., K.B. Jeganathan, J.F. Limzerwala, D.J. Baker, M. Hamada, H.-J.
882 Nam, W.H. van Deursen, N. Hamada, R.M. Naylor, N.A. Becker, B.A. Davies,
883 J.H. van Ree, G. Mer, V.S. Shapiro, L.J. Maher, D.J. Katzmann, and J.M. van
884 Deursen. 2016. Cyclin A2 is an RNA binding protein that controls Mre11
885 mRNA translation. *Science*. 353:1549–1552. doi:10.1126/science.aaf7463.

886 Katsuno, Y., A. Suzuki, K. Sugimura, K. Okumura, D.H. Zineldeen, M. Shimada, H.
887 Niida, T. Mizuno, F. Hanaoka, and M. Nakanishi. 2009. Cyclin A-Cdk1
888 regulates the origin firing program in mammalian cells. *Proc Natl Acad Sci U*
889 *A*. 106:3184–9. doi:10.1073/pnas.0809350106.

890 Kim, Y., N.G. Starostina, and E.T. Kipreos. 2008. The CRL4Cdt2 ubiquitin ligase targets
891 the degradation of p21Cip1 to control replication licensing. *Genes Dev*.
892 22:2507–19. doi:10.1101/gad.1703708.

893 Koundrioukoff, S., Z.O. Jónsson, S. Hasan, R.N. de Jong, P.C. van der Vliet, M.O.
894 Hottiger, and U. Hübscher. 2000. A direct interaction between proliferating
895 cell nuclear antigen (PCNA) and Cdk2 targets PCNA-interacting proteins for
896 phosphorylation. *J. Biol. Chem.* 275:22882–22887.
897 doi:10.1074/jbc.M001850200.

898 Krenning, L., F.M. Feringa, I.A. Shaltiel, J. van den Berg, and R.H. Medema. 2014.
899 Transient activation of p53 in G2 phase is sufficient to induce senescence.
900 *Mol Cell*. 55:59–72. doi:10.1016/j.molcel.2014.05.007.

901 Laoukili, J., M. Alvarez, L.A. Meijer, M. Stahl, S. Mohammed, L. Kleij, A.J. Heck, and
902 R.H. Medema. 2008. Activation of FoxM1 during G2 requires cyclin A/Cdk-
903 dependent relief of autorepression by the FoxM1 N-terminal domain. *Mol*
904 *Cell Biol*. 28:3076–87. doi:10.1128/MCB.01710-07.

905 Lemmens, B., N. Hegarat, K. Akopyan, J. Sala-Gaston, J. Bartek, H. Hochegger, and A.
906 Lindqvist. 2018. DNA Replication Determines Timing of Mitosis by Restricting
907 CDK1 and PLK1 Activation. *Mol Cell*. 71:117-128 e3.
908 doi:10.1016/j.molcel.2018.05.026.

909 Lemmens, B., and A. Lindqvist. 2019. DNA replication and mitotic entry: A brake
910 model for cell cycle progression. *J. Cell Biol.* 218:3892–3902.
911 doi:10.1083/jcb.201909032.

912 Li, J.-A., B.-C. Liu, Y. Song, and X. Chen. 2018. Cyclin A2 regulates symmetrical mitotic
913 spindle formation and centrosome amplification in human colon cancer cells.
914 *Am. J. Transl. Res.* 10:2669–2676.

915 Lindqvist, A., V. Rodriguez-Bravo, and R.H. Medema. 2009. The decision to enter
916 mitosis: feedback and redundancy in the mitotic entry network. *J Cell Biol*.
917 185:193–202. doi:10.1083/jcb.200812045.

918 Lukas, C., C.S. Sorensen, E. Kramer, E. Santoni-Rugiu, C. Lindeneg, J.M. Peters, J.
919 Bartek, and J. Lukas. 1999. Accumulation of cyclin B1 requires E2F and cyclin-
920 A-dependent rearrangement of the anaphase-promoting complex. *Nature*.
921 401:815–8. doi:10.1038/44611.

922 Macleod, K.F., N. Sherry, G. Hannon, D. Beach, T. Tokino, K. Kinzler, B. Vogelstein,
923 and T. Jacks. 1995. p53-dependent and independent expression of p21 during
924 cell growth, differentiation, and DNA damage. *Genes Dev*. 9:935–44.

925 Macurek, L., A. Lindqvist, D. Lim, M.A. Lampson, R. Klompmaker, R. Freire, C. Clouin,
926 S.S. Taylor, M.B. Yaffe, and R.H. Medema. 2008. Polo-like kinase-1 is activated
927 by aurora A to promote checkpoint recovery. *Nature*. 455:119–23.
928 doi:10.1038/nature07185.

929 Maridor, G., P. Gallant, R. Golsteyn, and E.A. Nigg. 1993. Nuclear localization of
930 vertebrate cyclin A correlates with its ability to form complexes with cdk
931 catalytic subunits. *J Cell Sci*. 106 (Pt 2):535–44.

932 Merrick, K.A., S. Larochelle, C. Zhang, J.J. Allen, K.M. Shokat, and R.P. Fisher. 2008.
933 Distinct activation pathways confer cyclin-binding specificity on Cdk1 and
934 Cdk2 in human cells. *Mol Cell*. 32:662–72. doi:10.1016/j.molcel.2008.10.022.

935 Mitra, J., and G.H. Enders. 2004. Cyclin A/Cdk2 complexes regulate activation of Cdk1
936 and Cdc25 phosphatases in human cells. *Oncogene*. 23:3361–7.
937 doi:10.1038/sj.onc.1207446.

938 Moore, J.D., J. Yang, R. Truant, and S. Kornbluth. 1999. Nuclear import of Cdk/cyclin
939 complexes: identification of distinct mechanisms for import of Cdk2/cyclin E
940 and Cdc2/cyclin B1. *J Cell Biol*. 144:213–24.

941 Müllers, E., H. Silva Cascales, K. Burdova, L. Macurek, and A. Lindqvist. 2017. Residual
942 Cdk1/2 activity after DNA damage promotes senescence. *Aging Cell*. 16:575–
943 584. doi:10.1111/acel.12588.

944 Mullers, E., H. Silva Cascales, H. Jaiswal, A.T. Saurin, and A. Lindqvist. 2014. Nuclear
945 translocation of Cyclin B1 marks the restriction point for terminal cell cycle
946 exit in G2 phase. *Cell Cycle*. 13:2733–43.
947 doi:10.4161/15384101.2015.945831.

948 Nishitani, H., Y. Shiomi, H. Iida, M. Michishita, T. Takami, and T. Tsurimoto. 2008.
949 CDK inhibitor p21 is degraded by a proliferating cell nuclear antigen-coupled
950 Cul4-DDB1Cdt2 pathway during S phase and after UV irradiation. *J Biol Chem*.
951 283:29045–52. doi:10.1074/jbc.M806045200.

952 Oakes, V., W. Wang, B. Harrington, W.J. Lee, H. Beamish, K.M. Chia, A. Pinder, H.
953 Goto, M. Inagaki, S. Pavey, and B. Gabrielli. 2014. Cyclin A/Cdk2 regulates
954 Cdh1 and claspin during late S/G2 phase of the cell cycle. *Cell Cycle*. 13:3302–
955 11. doi:10.4161/15384101.2014.949111.

956 Örd, M., and M. Loog. 2019. How the cell cycle clock ticks. *Mol. Biol. Cell*. 30:169–
957 172. doi:10.1091/mbc.E18-05-0272.

958 Pagano, M., R. Pepperkok, F. Verde, W. Ansorge, and G. Draetta. 1992. Cyclin A is
959 required at two points in the human cell cycle. *EMBO J*. 11:961–71.

960 Parrilla, A., L. Cirillo, Y. Thomas, M. Gotta, L. Pintard, and A. Santamaria. 2016.
961 Mitotic entry: The interplay between Cdk1, Plk1 and Bora. *Cell Cycle Georget.*
962 *Tex*. 15:3177–3182. doi:10.1080/15384101.2016.1249544.

963 Pechackova, S., K. Burdova, J. Benada, P. Kleiblova, G. Jenikova, and L. Macurek.
964 2016. Inhibition of WIP1 phosphatase sensitizes breast cancer cells to
965 genotoxic stress and to MDM2 antagonist nutlin-3. *Oncotarget*. 7:14458–
966 14475. doi:10.18632/oncotarget.7363.

967 Petersen, B.O., J. Lukas, C.S. Sorensen, J. Bartek, and K. Helin. 1999. Phosphorylation
968 of mammalian CDC6 by cyclin A/CDK2 regulates its subcellular localization.
969 *EMBO J*. 18:396–410. doi:10.1093/emboj/18.2.396.

970 Pines, J., and T. Hunter. 1991. Human cyclins A and B1 are differentially located in
971 the cell and undergo cell cycle-dependent nuclear transport. *J Cell Biol*.
972 115:1–17.

973 Pines, J., and T. Hunter. 1994. The differential localization of human cyclins A and B is
974 due to a cytoplasmic retention signal in cyclin B. *EMBO J*. 13:3772–81.

975 Qi, F., Q. Chen, H. Chen, H. Yan, B. Chen, X. Xiang, C. Liang, Q. Yi, M. Zhang, H. Cheng,
976 Z. Zhang, J. Huang, and F. Wang. 2018. WAC Promotes Polo-like Kinase 1
977 Activation for Timely Mitotic Entry. *Cell Rep.* 24:546–556.
978 doi:10.1016/j.celrep.2018.06.087.

979 Rodríguez-Vilarrupla, A., C. Díaz, N. Canela, H.P. Rahn, O. Bachs, and N. Agell. 2002.
980 Identification of the nuclear localization signal of p21(cip1) and consequences
981 of its mutation on cell proliferation. *FEBS Lett.* 531:319–323.
982 doi:10.1016/s0014-5793(02)03549-4.

983 Saldivar, J.C., S. Hamperl, M.J. Bocek, M. Chung, T.E. Bass, F. Cisneros-Soberanis, K.
984 Samejima, L. Xie, J.R. Paulson, W.C. Earnshaw, D. Cortez, T. Meyer, and K.A.
985 Cimprich. 2018. An intrinsic S/G2 checkpoint enforced by ATR. *Science*.
986 361:806–810. doi:10.1126/science.aap9346.

987 Seki, A., J.A. Coppinger, C.-Y. Jang, J.R. Yates, and G. Fang. 2008. Bora and the kinase
988 Aurora a cooperatively activate the kinase Plk1 and control mitotic entry.
989 *Science*. 320:1655–1658. doi:10.1126/science.1157425.

990 Sheng, C., I.-H. Mendler, S. Rieke, P. Snyder, M. Jentsch, D. Friedrich, B. Drossel, and
991 A. Loewer. 2019. PCNA-Mediated Degradation of p21 Coordinates the DNA
992 Damage Response and Cell Cycle Regulation in Individual Cells. *Cell Rep.*
993 27:48-58.e7. doi:10.1016/j.celrep.2019.03.031.

994 Sørensen, C.S., and R.G. Syljuåsen. 2012. Safeguarding genome integrity: the
995 checkpoint kinases ATR, CHK1 and WEE1 restrain CDK activity during normal
996 DNA replication. *Nucleic Acids Res.* 40:477–486. doi:10.1093/nar/gkr697.

997 Swaffer, M.P., A.W. Jones, H.R. Flynn, A.P. Snijders, and P. Nurse. 2016. CDK
998 Substrate Phosphorylation and Ordering the Cell Cycle. *Cell*. 167:1750-
999 1761.e16. doi:10.1016/j.cell.2016.11.034.

1000 Takizawa, C.G., and D.O. Morgan. 2000. Control of mitosis by changes in the
1001 subcellular location of cyclin-B1-Cdk1 and Cdc25C. *Curr Opin Cell Biol*.
1002 12:658–65.

1003 Taniguchi, E., F. Toyoshima-Morimoto, and E. Nishida. 2002. Nuclear translocation of
1004 plk1 mediated by its bipartite nuclear localization signal. *J. Biol. Chem.*
1005 277:48884–48888. doi:10.1074/jbc.M206307200.

1006 Tavernier, N., A. Noatynska, C. Panbianco, L. Martino, L. Van Hove, F. Schwager, T.
1007 Léger, M. Gotta, and L. Pintard. 2015. Cdk1 phosphorylates SPAT-1/Bora to
1008 trigger PLK-1 activation and drive mitotic entry in C. elegans embryos. *J. Cell*
1009 *Biol.* 208:661–669. doi:10.1083/jcb.201408064.

1010 Thomas, Y., L. Cirillo, C. Panbianco, L. Martino, N. Tavernier, F. Schwager, L. Van
1011 Hove, N. Joly, A. Santamaria, L. Pintard, and M. Gotta. 2016. Cdk1
1012 Phosphorylates SPAT-1/Bora to Promote Plk1 Activation in C. elegans and
1013 Human Cells. *Cell Rep.* 15:510–518. doi:10.1016/j.celrep.2016.03.049.

1014 Thul, P.J., L. Åkesson, M. Wiking, D. Mahdessian, A. Geladaki, H. Ait Blal, T. Alm, A.
1015 Asplund, L. Björk, L.M. Breckels, A. Bäckström, F. Danielsson, L. Fagerberg, J.
1016 Fall, L. Gatto, C. Gnann, S. Hober, M. Hjelmare, F. Johansson, S. Lee, C.
1017 Lindskog, J. Mulder, C.M. Mulvey, P. Nilsson, P. Oksvold, J. Rockberg, R.

1018 Schutten, J.M. Schwenk, Å. Sivertsson, E. Sjöstedt, M. Skogs, C. Stadler, D.P.
1019 Sullivan, H. Tegel, C. Winsnes, C. Zhang, M. Zwahlen, A. Mardinoglu, F.
1020 Pontén, K. von Feilitzen, K.S. Lilley, M. Uhlén, and E. Lundberg. 2017. A
1021 subcellular map of the human proteome. *Science*. 356.
1022 doi:10.1126/science.aal3321.

1023 Trembecka-Lucas, D.O., D.O. Trembecka-Lucas, A.T. Szczurek, A.T. Szczurek, J.W.
1024 Dobrucki, and J.W. Dobrucki. 2013. Dynamics of the HP1β-PCNA-containing
1025 complexes in DNA replication and repair. *Nucleus*. 4:74–82.
1026 doi:10.4161/nucl.23683.

1027 Tsang, W.Y., L. Wang, Z. Chen, I. Sanchez, and B.D. Dynlacht. 2007. SCAPER, a novel
1028 cyclin A-interacting protein that regulates cell cycle progression. *J Cell Biol*.
1029 178:621–33. doi:10.1083/jcb.200701166.

1030 Uetake, Y., and G. Sluder. 2010. Prolonged prometaphase blocks daughter cell
1031 proliferation despite normal completion of mitosis. *Curr. Biol. CB*. 20:1666–
1032 1671. doi:10.1016/j.cub.2010.08.018.

1033 Vigneron, S., L. Sundermann, J.-C. Labbé, L. Pintard, O. Radulescu, A. Castro, and T.
1034 Lorca. 2018. Cyclin A-cdk1-Dependent Phosphorylation of Bora Is the
1035 Triggering Factor Promoting Mitotic Entry. *Dev. Cell*. 45:637-650.e7.
1036 doi:10.1016/j.devcel.2018.05.005.

1037 Woodman, P.G., J.P. Adamczewski, T. Hunt, and G. Warren. 1993. In vitro fusion of
1038 endocytic vesicles is inhibited by cyclin A-cdc2 kinase. *Mol Biol Cell*. 4:541–53.

1039

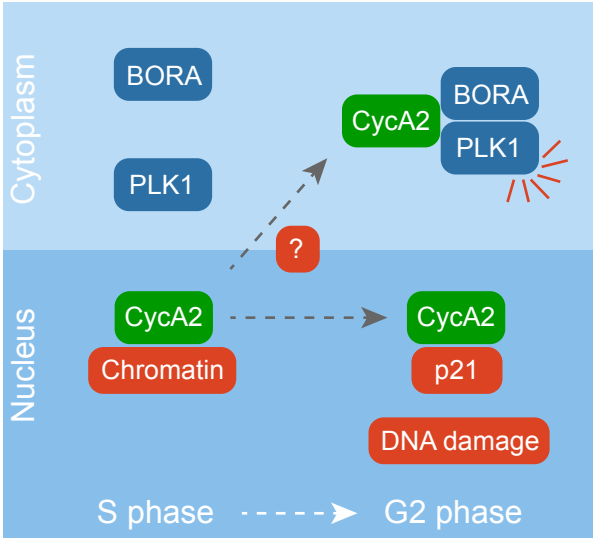

Silva Cascales et al. Graphical abstract

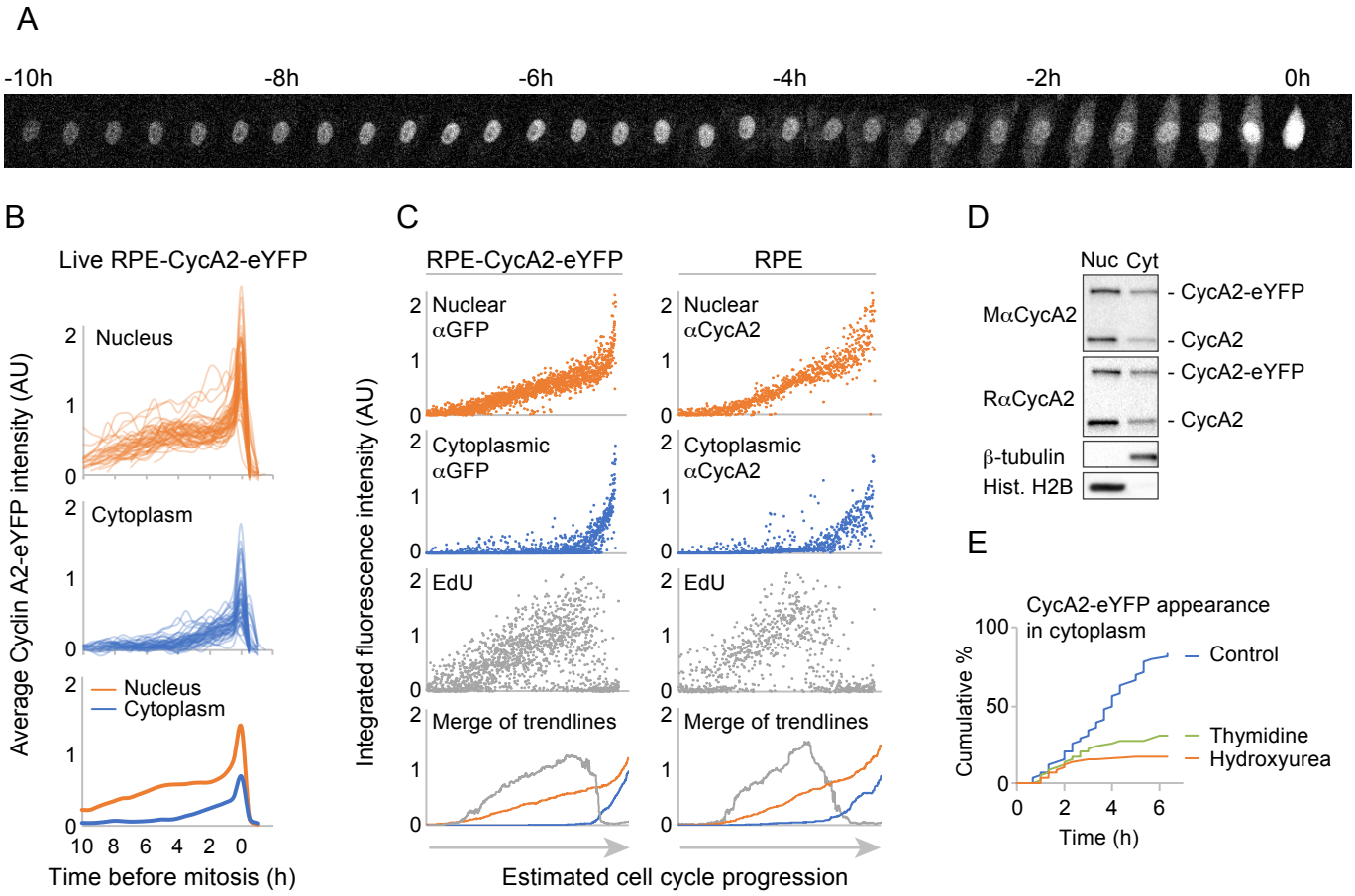

Figure 1. Silva Cascales et al

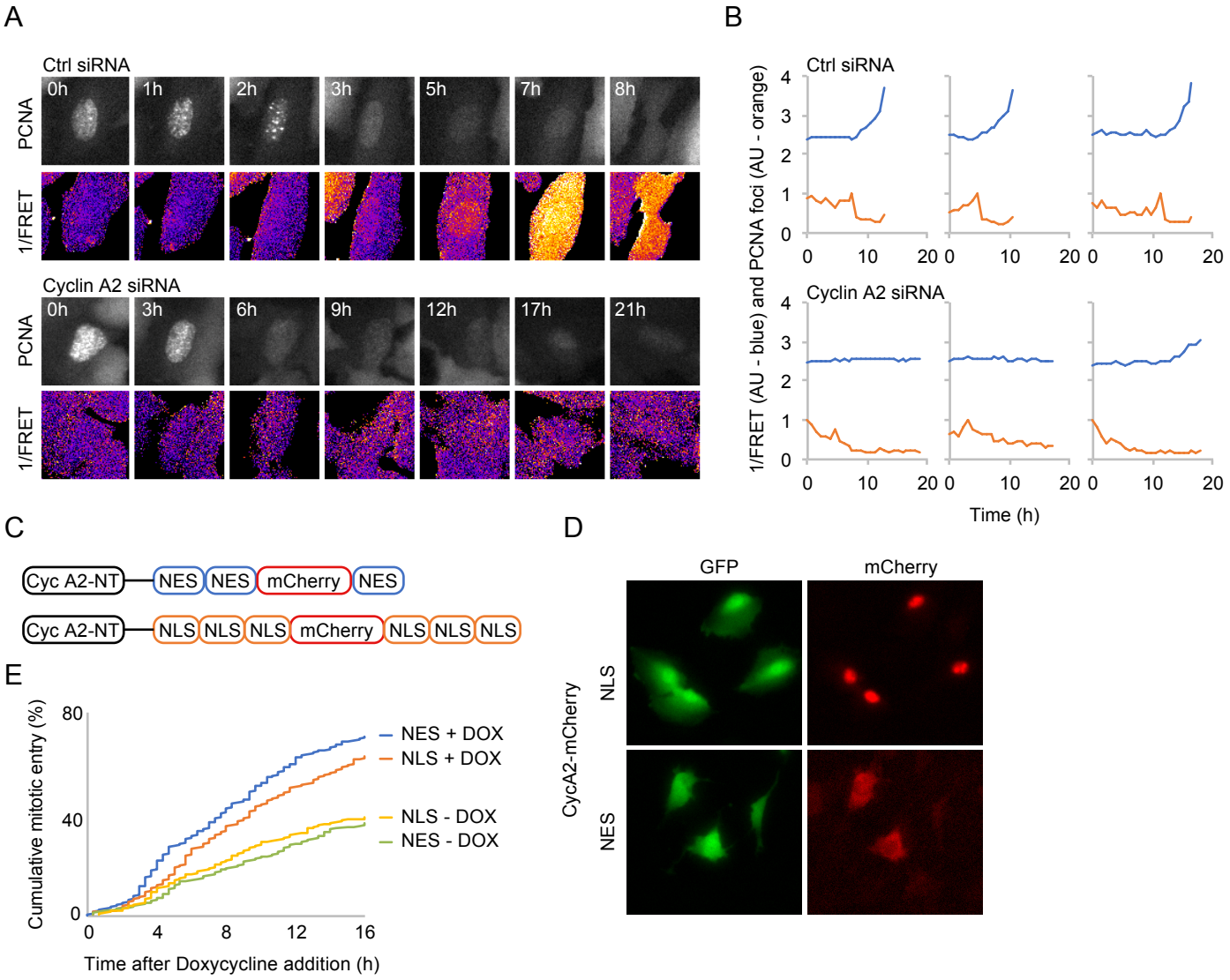

Figure 2. Silva Cascales et al

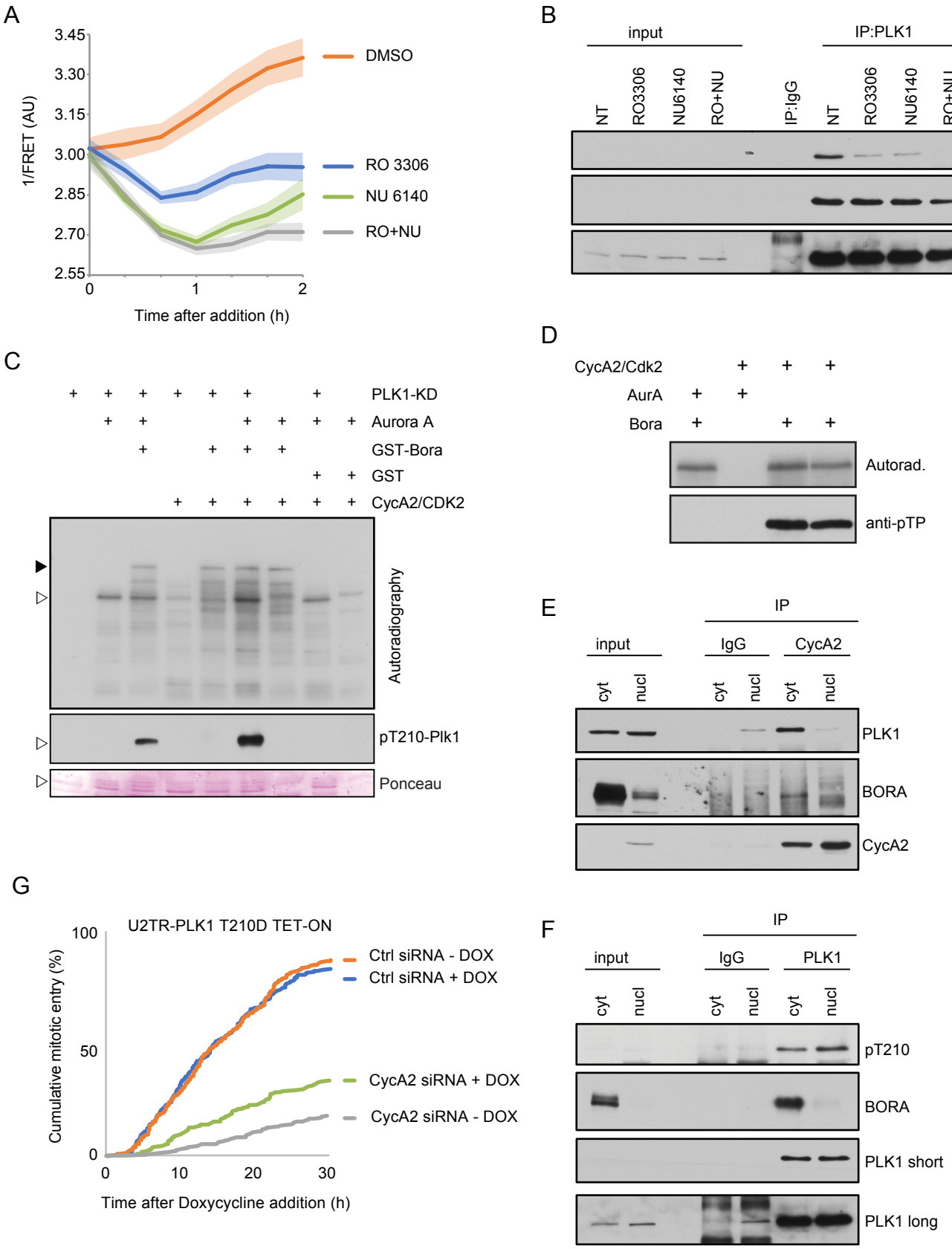

Figure 3. Silva Cascales et al

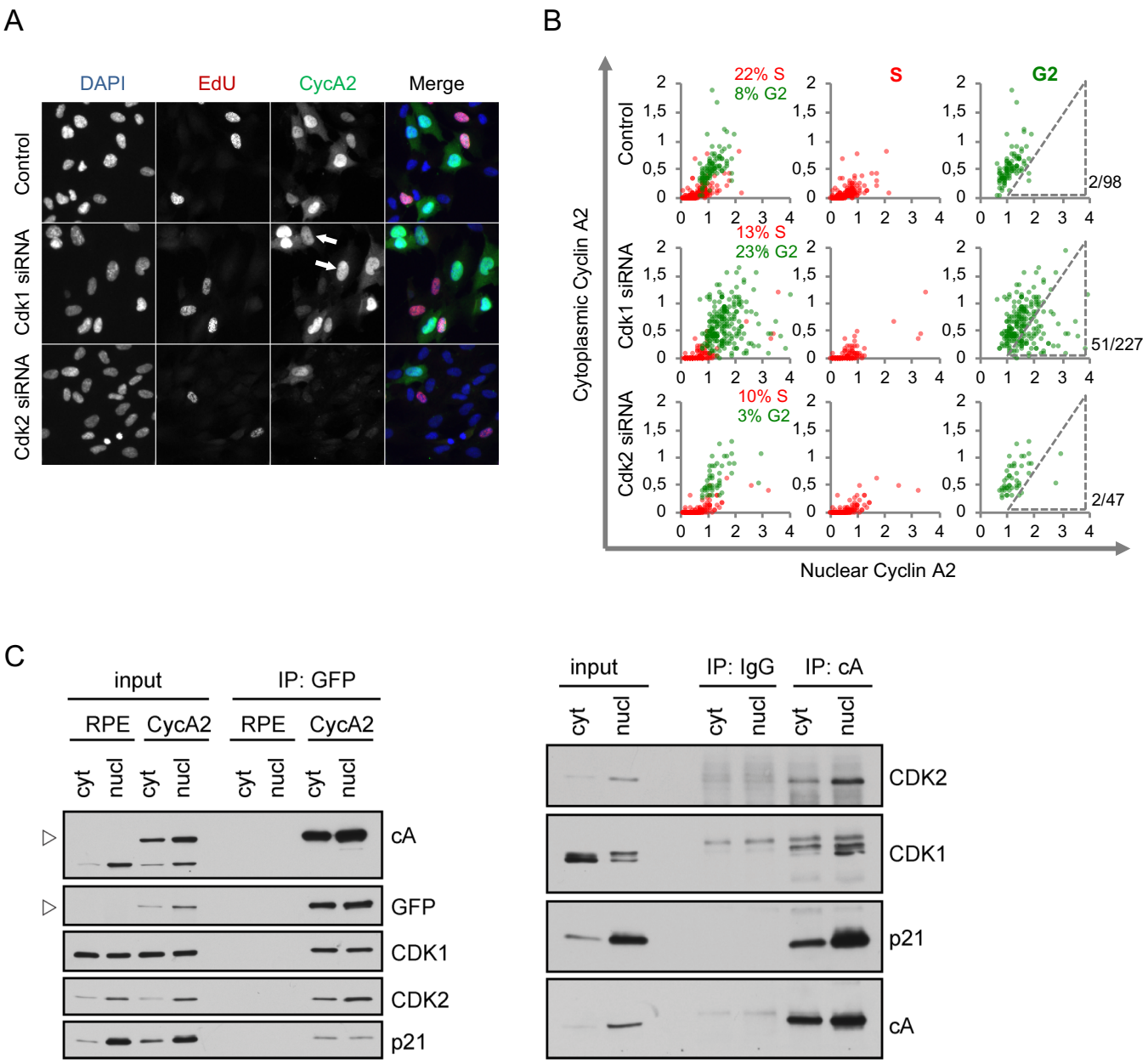

Figure 4. Silva Cascales et al

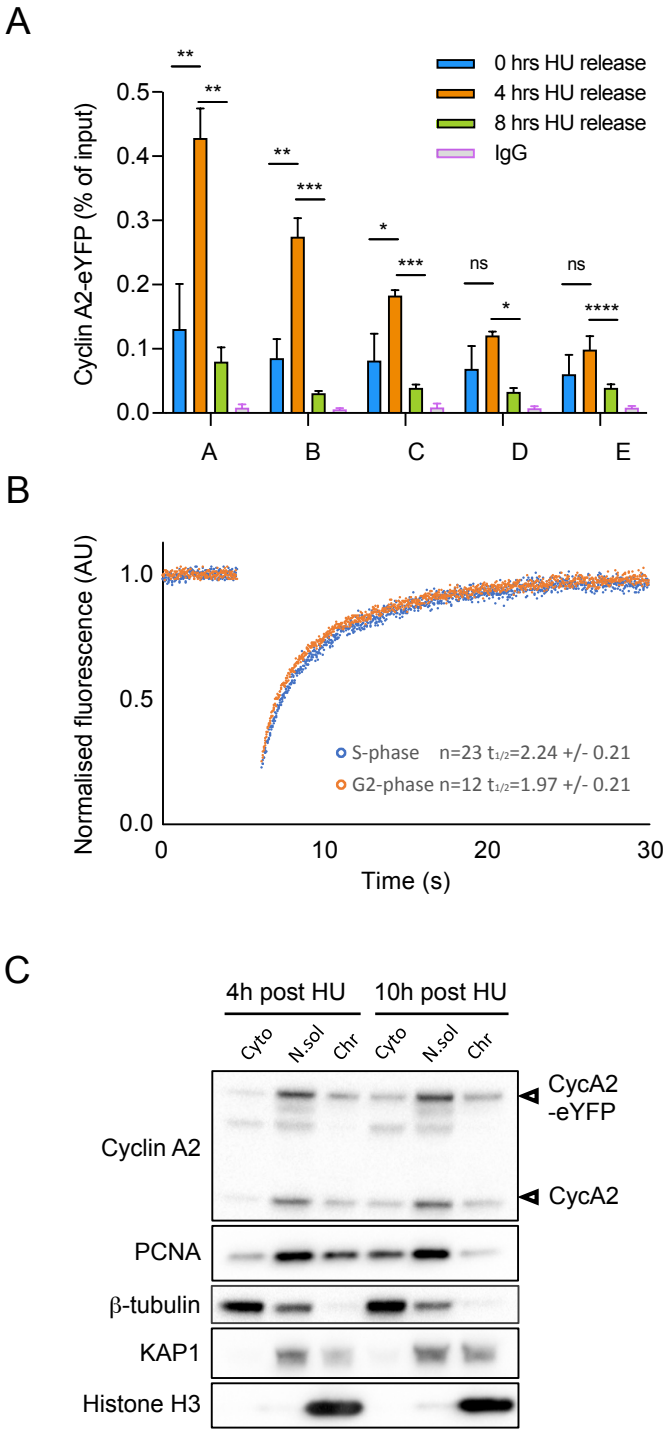

Figure 5. Silva Cascales et al.

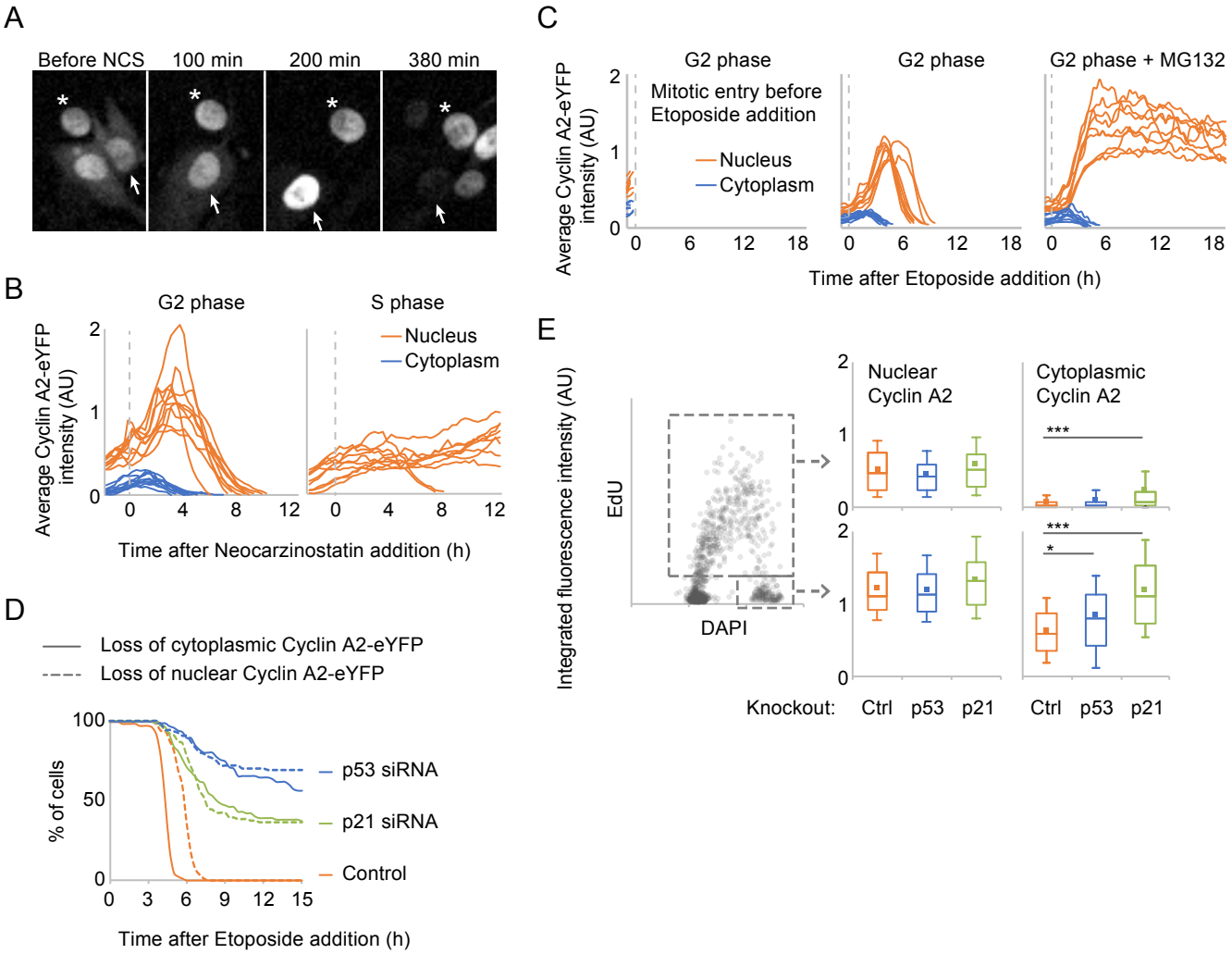

Figure 6. Silva Cascales et al

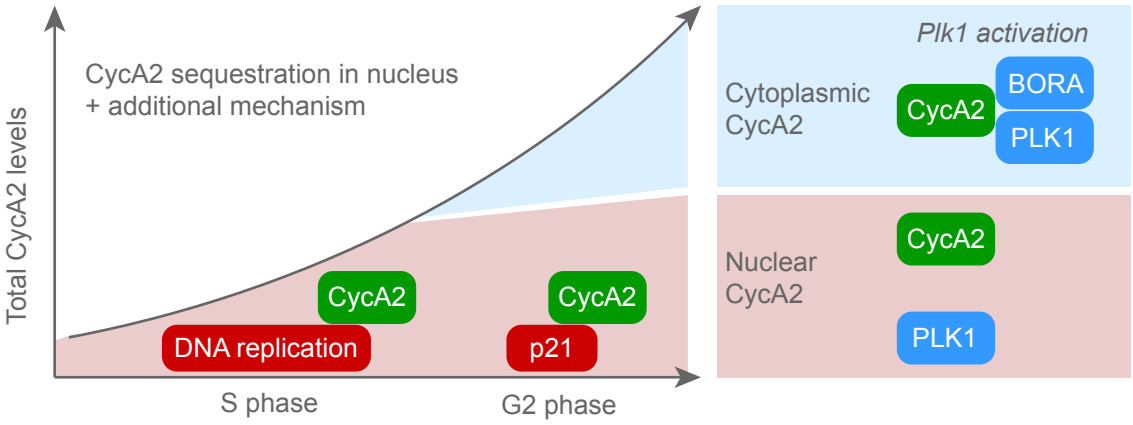

Figure 7. Silva Cascales et al

Supplementary Figure 1

a

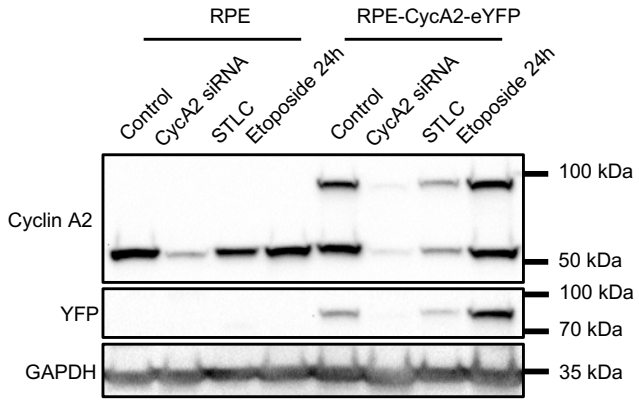

b

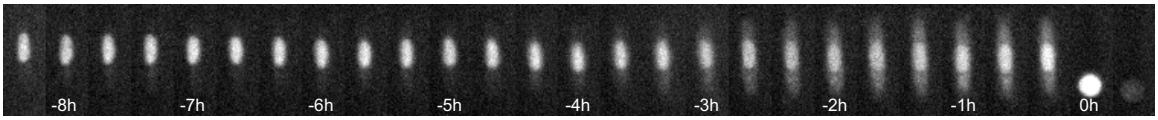

c

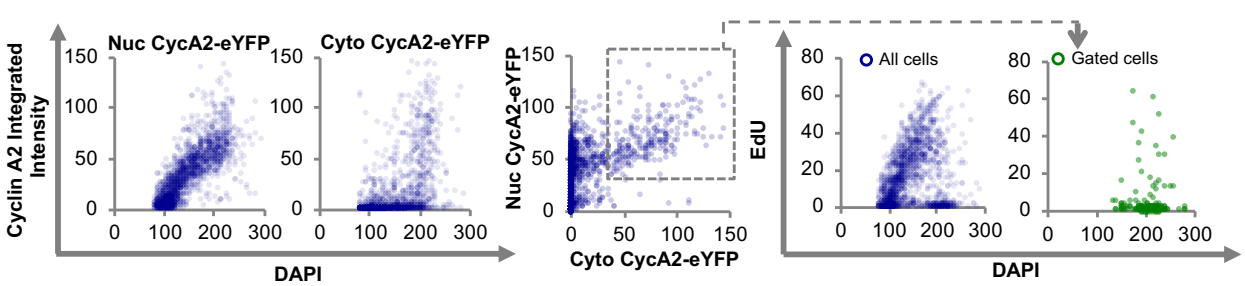

d

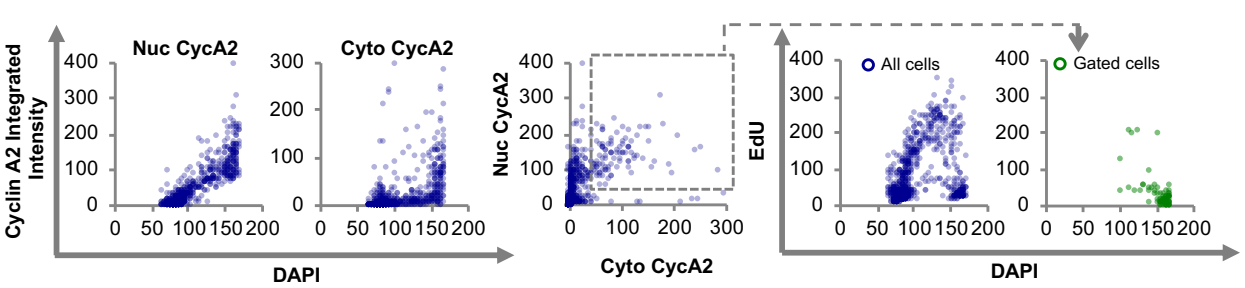

Supplementary Figure 2

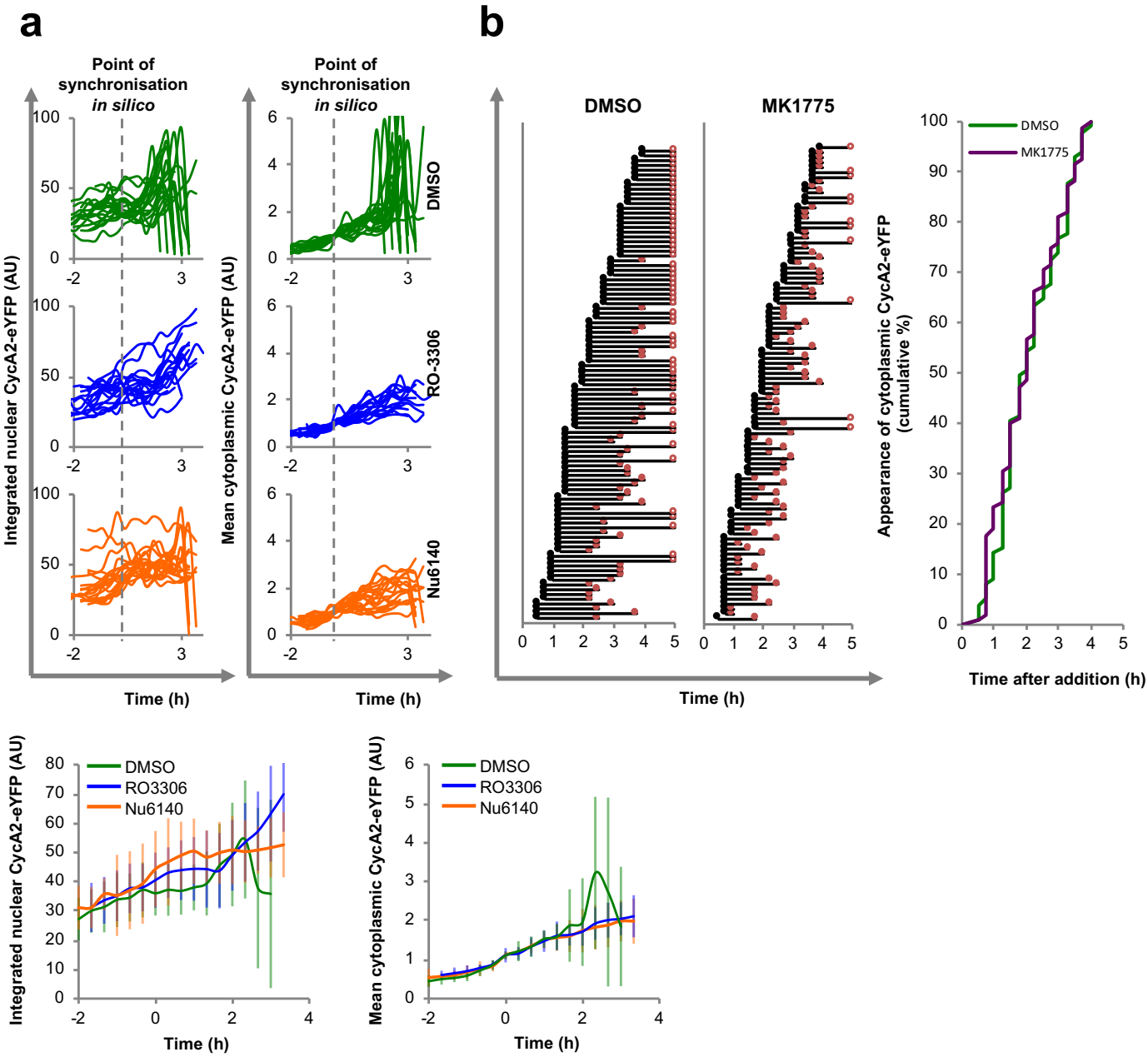

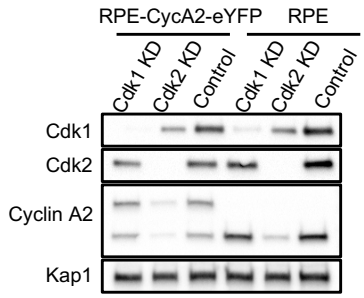

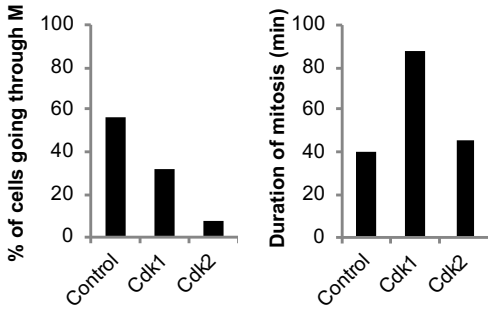

Supplementary Figure 3

a

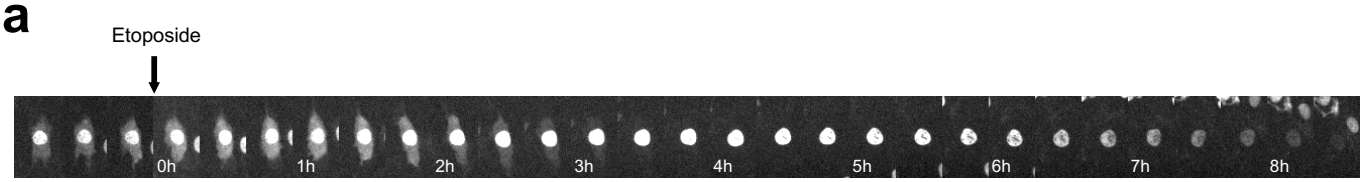

b

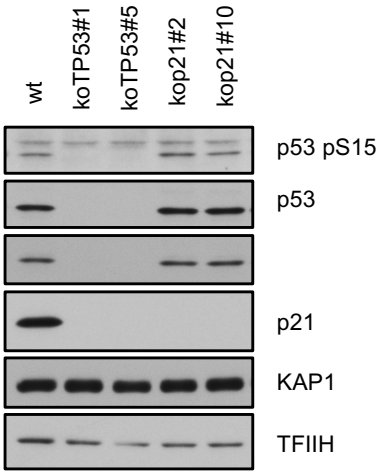

Supplementary Table 1

Name	Gene	Forward primer 5’>3’	Reverse Primer 5’>3’
A	MYC	GGACTCAGTCTGGGTGGAAGG	AAGGAGGAAAACGATGCCTAGA
B	IRF1	GGGAGGGTTTCAGTCCTAGC	CCATCACAGCAAACCATCAA
C	LAMB2	CCAGAATCCGATCATGCACC	TCCGTTTTTGCAGGTTGTGCT
D	α-satellite DNA	CTTTTTCATCATAGGCCTCAA	AGCTCACAGAGCTGAAACATT
E	Intergenic Chr1	GCAGTTCAACCTACAAGCCAATAGAC	CACAAATTAGCGCATTGCCTGA